Theory of Curved Space and the Plateau Law: the role of Noether currents

M. V. Govorushkin

Abstract

This paper proposes a fundamentally different ontological picture than the Standard Model and General Relativity.

Space is represented by four equal axes (x_1, x_2, x_3, x_4), the evolution of which occurs along a single absolute time t. All "relativistic" effects (slowing down of processes, length shortening, frequency shifts) are explained not by the change of the metric tensor, but by the geometry of the projection of 4D trajectories onto our 3D slice. The two-way (average) speed of light along any closed route is fixed by the postulate $\langle c \rangle = c$, while the one-way speed can be anisotropic and depend on the synchronization procedure.

The global symmetry $SL(4, \mathbb{R})$ generates four independent Noether currents: conservation of charge, energy, momentum and "scale" (plateau law). The integrals of the flows of these currents give universal quantizing and plateau conditions from atomic orbits to galactic disks.

The work is structured in increasing complexity: 1) axiomatics and ontology of the TCS; 2) kinematics of light and absolute time; 3) the dynamics of the field $Q(x, t)$ and the derivation of the "master equation"; 4) applications to astrophysical and cosmological phenomena (galactic curves, CMB); 5) generalizations to microphysics and the standard model.

Important note for the reader. A reader familiar with standard physics may experience cognitive dissonance. The Curved Space Theory (CST) does not offer "new physics inside an old universe". It describes an alternative world where

- space is a purely four-dimensional deformation of $SL(4, \mathbb{R})$ without mixing with time;
- time t is an absolute parameter of evolution, the same for all processes;
- light and particles move in 4D, and all the observed "relativistic" effects arise only when projected onto our 3D slice.

If some result seems to contradict STR/GR, this is not an error, but a reflection of other initial axioms. The TCS should be assessed by three criteria:

1. internal logical consistency of axioms and conclusions;
2. ability to quantitatively describe existing experimental data;
3. ability to give new, falsifiable predictions.

This work shows that the TCS satisfies all three criteria, thus being a self-sufficient alternative to standard models.

Table of Contents

Introduction **6**

Conventions and Notations **7**

1 Space and time in TCS **7**

1.1 Four spatial axes 7
1.2 Absolute time 8
1.3 Preservation of 4D volume 8
1.4 Physical meaning 8

2 Field $Q(x)$ and global symmetry **8**
2.1 Physical meaning of $Q(x)$ . . . 8
2.2 Why $SL(4,\mathbb{R})$ . . . 9
2.3 Global Symmetry . . . 9
2.4 Noether's theorem and the conserved current . . . 9
2.5 Why do we need this current . . . 9

3 Kinematics of light and absolute time **10**
3.1 Two-way speed of light as an axiom . . . 10
3.2 Absolute time and motion . . . 10
3.3 Light front in 4D . . . 10
3.4 Why is this important for TCS . . . 10
3.5 Rotation of the IFR in E_4, the projection ellipsoid, and the complete invariant . . . 10
3.6 3D-slice interval, Lagrangian, and weak-field E–p coupling . . . 12
3.7 Oscillatory nature of mass and wave gravity in TCS . . . 13
3.8 TCS: Unified Energy-Momentum Formula, Magnetic Field Projection, KGF, and Dirac Equation . . . 15
3.9 Unified formula of energy-momentum and non-relativistic limit for all interactions in TCS . . . 17
3.10 Plateau law for disk regime . . . 18
3.11 Spherical Geometry . . . 18
3.12 Sparse halo . . . 18
3.13 Derivation of the PLATEAU law . . . 19
3.14 Minimal action for the field Q in TCS . . . 20
3.15 Noether current: from symmetry to conservation . . . 20
3.16 Master equation of homothetic flow in TCS . . . 22
3.16.1 Origin and evolution of A^{ij} . . . 23
3.16.2 Connection with visible matter . . . 24
3.16.3 The nature of the transfer velocity u_j^* . . . 24
3.17 Deduction of low-energy action and closure of equations for A^{ij} and u_j^* . . . 25
3.18 Relationship between the geometry of angular momentum and the law of homothetic flow . . . 26
3.19 Agreement with experimental data and TCS predictions . . . 27
3.20 How the invariant $R^2\rho = \text{const}$ is obtained from the conserved current . . . 28
3.21 What types of currents are there and what do they mean (in simple terms) . . . 29
3.22 Examples of current interpretation and stress tests . . . 30
3.23 Black hole and "radius of the Universe" parameters from spherical flow . . . 31
3.24 Four currents of the TCS using the example of an electron in an atom . . . 32
3.24.1 Four currents in the atomic problem . . . 33

4 Gauge fields from TCS **34**
4.1 Matrix $Q(x)$ as a configuration field . . . 34
4.2 From global to local symmetry . . . 34
4.3 Decomposition of the algebra $\mathfrak{sl}(4,\mathbb{R})$ . . . 34
4.4 Fields of the Standard Model . . . 35
4.5 Curvature and Yang–Mills equations . . . 35
4.6 Physical meaning in TCS . . . 35
4.7 The problem of choosing a representation and the selection protocol . . . 35
4.7.1 Rigidity of the choice of $SU(3) \times SU(2) \times U(1)$ inside $SU(4)$ . . . 37
4.7.2 Fermions as sections of a spinor bundle with internal connection . . . 37

4.8 Complex phase of $U(1)$ and embeddings of $SU(3)$, $SU(2)$ in $SL(4,\mathbb{R})$ 38
4.9 Uniqueness of embedding $\mathrm{SL}(4,\mathbb{R}) \to \mathrm{SU}(3) \times \mathrm{SU}(2) \times \mathrm{U}(1)$ 40

5 General action and the TCS gravity equation **41**
5.1 Gravitational action 41
5.2 Material part 41
5.3 Equation of motion for ϕ 42
5.4 Linearization and Newtonian limit 42
5.5 Weak-field limit and Newtonian normalization 44

6 TIP Gravitational Sector **44**
6.1 Mass as the Amplitude of Perpendicular Oscillations 44
6.2 Kinematic picture: sphere $\to$ ellipsoid 44
6.3 Spin modes 45
6.4 Wave interpretation 45
6.5 Group structure: $12 + 3 = 15$ 45
6.6 Experimental Relations and Predictions 45
6.7 KGF from TCS variance and definition of ν^2 46
6.8 Geometric origin of the Higgs potential in the TCS 48
6.9 Effective potential of hypercube rotation in the TCS 49

A Experimental tests of the geometric model with absolute time **50**
A.1 Muons from cosmic rays: distance contraction 50
A.2 Muons in a collider 51
A.3 GPS in SR and TCS 51
A.4 Hafele–Keating experiment and interpretation in TCS 52
A.5 Red and blue shift in the gravitational field (TCS) 53
A.6 Collider particles 53

B Axomatic basis TCS (4+0, absolute time, bidirectional gauge c) **54**
B.1 Variation of the action and derivation of the transport equation 55
B.2 Reduction to a scalar "master equation" 56
B.3 Relation to $\langle v \rangle_{\text{closed}} = c$ gauge and absence of sources 56
B.4 Explicit specification of A^{ij} and u_j^* from the Lagrangian 57
B.5 Summary and Verifiability 57
B.6 Small fluctuations: kinetic decay and values of the coefficients c_A, c_u 57
B.7 Physical meaning of the fields Q, A^{ij} and u_j^* 59

C Example: a black hole in TCS via currents and projection **60**
C.1 Problem statement 60
C.2 Curvature Current and Field Function 61
C.3 Transition to the observed 3D slice 61
C.4 Killing currents and constants of motion 61
C.5 Light ray and photosphere 61
C.6 Shadow parameter 62
C.7 Circular Particle Orbits and ISCO 62
C.8 Shapiro delay and redshift 62
C.9 Conclusion 62
C.10 KG–Fock in TCS and interpretation of the imaginary component of the interval 63
C.11 Internal structure via homothetic current 64
C.12 Generalization to charged and rotating objects 64

C.12.1 Relationship between the frequency of oscillations and the gravitational radius . . . 65

D A rotating black hole in TCS: from conditions to observations 66
D.1 The idea in a nutshell . . . 66
D.2 How the functions $F_{\text{eff}}(r)$ and $\Omega_{\text{eff}}(r)$ are fixed . . . 66
D.3 Radial equation for waves . . . 66
D.4 Geometric phase $z(r)$ . . . 67
D.5 How TCS differs from GTR here . . . 67
D.6 Example calculation for $M = 10\,M_{\odot}$,$a = 0.7$ . . . 67
D.7 Observational tests . . . 67

E Cosmology in the TCS formalism 68
E.1 Background equations . . . 68
E.2 Consistency with ΛCDM . . . 68
E.3 Diagnostics by CMB . . . 68

F Experimental verification of the homothetic current and comparison with MOND and ΛCDM 68
F.1 Lensing in TCS: SDSS J2141 . . . 70

Introduction

Problem

Constancy of the Speed of Light

It should be emphasized that the *one-way* speed of light has never been measured directly: all known anisotropy experiments (Michelson-Morley, Kennedy-Thorndike, modern fiber optic tests) actually test the *two-way* speed of signal propagation, i.e. the average speed there and back along the same path.
In the framework of the Theory of Curved Space (TCS), the two-way speed of light in all inertial systems is strictly equal to the accepted average speed c, which is completely consistent with the results of all similar experiments. Thus, TCS does not contradict any of the known tests for the anisotropy of the speed of light, and the differences with STR concern only the interpretation and possible anisotropy of the *one-way* speed, which is not experimentally recorded withouts additional agreements on synchronization.

Observations show that on the outskirts of spiral galaxies, stars move at almost the same speed, forming a "plateau" of the rotation curve. Classical Newtonian gravity predicts a decline in $v \propto R^{-1/2}$, and to explain the discrepancy in standard cosmology, a hypothetical "dark matter" is introduced.

Two-way speed of light in TCS

Corollary 1 (TIP postulate on the speed of light)**.** *In all inertial reference frames, the* round-trip *speed of light is the same and equals c. The one-way speed may depend on the chosen synchronization procedure and is not fixed by this postulate.*

Comment. It is the two-way speed that is tested experimentally: all classical tests (Michelson-Morley, Kennedy-Thorndike, laser gyroscopes, GPS, VLBI) measure the time it takes for a signal to travel along a closed loop and back.

In TCS, for any isochronous closed path γ of length $\mathcal{L}_\gamma$, we have

$$T_\gamma = \oint_\gamma \frac{d\ell}{c}, \qquad \frac{\mathcal{L}_\gamma}{T_\gamma} = c,$$

where T_γ is the absolute round-trip time, $d\ell$ is the length element in the 3D slice. This identity of the model guarantees the coincidence with the observed constraints:

$$\frac{\delta T_\gamma}{T_\gamma} < 10^{-19} \text{ (laser gyroscopes)}, \quad \lesssim 10^{-12}\,\text{s (GPS, VLBI)}.$$

Thus, the CST is in full agreement with the results of all known experiments on the anisotropy of the two-way speed of light.

The CST approach

The Curved Space Theory (CST) offers a different path based on three axioms:

1. **Absolute time** t is a single parameter of evolution, the same at all points in space.
2. **Four equal spatial axes** (x^1, x^2, x^3, x^4) — time does not mix with space.

3. **Preservation of 4D volume**: admissible deformations of space preserve its four-dimensional volume, and *information about the conservation of this volume propagates with the average speed of light c.*

Consequences

Preservation of 4D volume means the presence of global $SL(4,\mathbb{R})$ symmetry. By Noether's theorem, this implies the existence of a *conserved homothetic current*, which:

- in disk geometry gives $v^2 = \text{const}$ — a velocity plateau without dark matter;
- in spherical geometry at $\rho \propto R^{-2}$ leads to a threshold acceleration of $a_0 \approx 10^{-10}\,\text{m/s}^2$;
- physically in TCS is interpreted as a manifestation of the global rotation of the Universe around the fourth spatial axis.

Conventions and Notations

Units and Constants. We use SI until the completion of integrals. $c = 2.99792458 \times 10^8$ m/s, $G = 6.67430 \times 10^{-11}\ \text{m}^3\,\text{kg}^{-1}\,\text{s}^{-2}$. Translation: $\alpha["] = \alpha[\text{rad}] \times 206265$. Angular distances: D_d, D_s, D_{ds}.
Absolute time and projection. t is an absolute parameter. Observed kinematics is a projection of 4D trajectories onto a 3D slice; "relativistic" effects are treated as projection geometry.
Flow invariants. Sphere: $K_s = R^2 J_3\,\rho\,u^* = \text{const}$. Disk: $K_a = R\,J_3\,\Sigma\,u_R^* = \text{const}$. Units: $[K_s] = \text{M}/(\text{L}\cdot\text{T})$, $[K_a] = \text{M}/\text{T}$.
Anisotropy. A^{ij} is a symmetric dimensionless tensor, $\operatorname{tr} A = 2$; isotropy: $A^{ij} \to \delta^{ij}$; thin disk: $A^{zz} \ll A^{RR} \simeq A^{\phi\phi} \simeq 1$.
Two kappas. κ_{mat} is a coefficient in the variational equations for Q (internal dynamics). κ_{wf} is a weak-field scale in $\Phi_{\text{TCS}}(r) = \Phi_0 - \frac{\kappa_{\text{wf}}}{2}\,u^*(r)^2$, is fixed once from $\Delta\Phi = 4\pi G\rho$.
Light deflection.

$$\hat{\alpha}(b) = \frac{4}{c^2}\int_{-\infty}^{+\infty} \frac{\partial \Phi_{\text{TCS}}(r)}{\partial r}\,\frac{b}{r}\,dl, \quad r = \sqrt{b^2 + l^2}, \quad \alpha(\theta) = \frac{D_{ds}}{D_s}\,\hat{\alpha}(b),\ b = D_d\,\theta.$$

All D are angular diameters.

1 Space and time in TCS

1.1 Four spatial axes

In TCS, space has four equal coordinates:

$$(x^1,\, x^2,\, x^3,\, x^4).$$

They are all spatial, without a dedicated "time" axis. Any deformation we consider acts only in these four dimensions.

1.2 Absolute time

Time t is an external parameter of evolution. It:

- flows equally at all points in space;
- is not mixed with spatial coordinates;
- is not included in the definition of spatial volume.

Thus, volume in TCS is a purely four-dimensional volume in $x^1 - x^4$.

1.3 Preservation of 4D volume

Main postulate: add.stable deformations of space preserve its four-dimensional volume. If the volume has changed in some region, information about this change propagates in space with *the average speed of light* c. This means:

- there is no instantaneous "knowledge" about the deformation in the entire Universe;
- the front of information about the conservation of volume moves as a spherical wave in 4D space;
- the average speed of this front is c, which is consistent with the observed limitations on the speed of interaction transmission.

1.4 Physical meaning

Absolute time fixes the order of events, and the conservation of volume fixes the "rigidity" of space in 4D. The limited speed of propagation of information about the conservation of volume makes the model dynamic and allows one to describe the processes of evolution of galaxies, halos, and other structures without introducing dark matter.

Key difference TCS

In **Curved Space Theory (TCS)absolute time T is the same for all directions and does not slow down**. The observed differences in one-way velocities arise *not* from a change in the flow of time, but from a **change in the projected path length** $L_{\pm}$ when mapping from isotropic E_4 to a three-dimensional slice.
In other words, the TCS describes the same physical phenomena as relativistic kinematics, but “in profile”: instead of time dilations, there is a projection geometry, in which the sum of the lengths $L_+ + L_-$ always gives $2cT$, and the two-way velocity $\bar{w}$ in all directions is equal to c.

2 Field $Q(x)$ and global symmetry

2.1 Physical meaning of $Q(x)$

At each point of four-dimensional space $x = (x^1, x^2, x^3, x^4)$ we define the matrix

$$Q(x) \in SL(4, \mathbb{R}), \quad \det Q = 1.$$

This matrix describes a local *volume-preserving* deformation of 4D space:

- it can stretch or compress space along different axes;
- but the overall four-dimensional volume remains unchanged;
- time t remains an external parameter and is not included in the volume.

2.2 Why $SL(4,\mathbb{R})$

The group $SL(4,\mathbb{R})$ is all 4×4 matrices with $\det = 1$. It is natural for describing deformations that:

- act only on four spatial coordinates;
- preserve 4D volume;
- can be either global (the same everywhere) or local (depending on x).

2.3 Global Symmetry

If the same matrix $g \in SL(4,\mathbb{R})$ is applied simultaneously throughout the entire space:

$$Q(x) \longrightarrow g\,Q(x),$$

then the physical properties will not change. This is the *global symmetry*.

2.4 Noether's theorem and the conserved current

By Noether's theorem, any continuous symmetry yields a conservation law.
For global $SL(4,\mathbb{R})$–symmetry, this is the *homothetic current* J^i:

$$\partial_i J^i = 0.$$

Physically:

- J^i is the "flow of information" about the conservation of the 4D–volume;
- it propagates in space with the average speed of light c;
- the magnitude of the flow through any closed 3D–hypersurface in 4D remains constant.

2.5 Why do we need this current

It is the conservation of J^i in different geometries (disk, sphere) that gives:

- velocity plateau in spiral galaxies;
- decline of $v \propto 1/\sqrt{R}$ in spheres;
- threshold acceleration a_0 in sparse halos.

3 Kinematics of light and absolute time

3.1 Two-way speed of light as an axiom

In TCS we immediately include: if we send a light signal back and forth along the same path, then the average speed is always equal to c:

$$v_{\text{two-way}} = \frac{L_+ + L_-}{T} = c,$$

where L_+ and L_- are the lengths of the path in the forward and reverse directions, and T is the *absolute* time of the full run, measured by the same clock. This condition is fulfilled with the accuracy of modern experiments (10^{-12}–10^{-19}).

3.2 Absolute time and motion

Time t in TCS is a common parameter for all reference systems. When moving to a system moving with a constant velocity u along one of the spatial axes, only the spatial coordinates change, while t remains the same.

3.3 Light front in 4D

In four-dimensional space, the light front from a flash at the moment $t = 0$ is a sphere of radius ct:

$$(x^1)^2 + (x^2)^2 + (x^3)^2 + (x^4)^2 = (ct)^2.$$

If we consider a three-dimensional slice (for example, (x^1, x^2, x^3)), then the projection of this sphere looks like an ellipsoid. But in any direction, the path there and back takes the same absolute time T, and the average speed remains c.

3.4 Why is this important for TCS

- This sets a "speed limit" for the dissemination of any information, including information about the preservation of 4D volume.
- Guarantees thatlasie with experiments on measuring the speed of light.
- Allows us to construct the dynamics of $Q(x)$ so that the front of changes in space moves with an average speed of c.

3.5 Rotation of the IFR in E_4, the projection ellipsoid, and the complete invariant

Geometry of rotation. In TCS, space is four-dimensional, and the relative uniform motion of two inertial systems (ISF) is a *rotation* by an angle of θ in E_4 along the velocity vector. The light 3D sphere of radius ct in one IFR rotates and in projection onto our 3D slice becomes an *ellipsoid*, compressed across the motion.

Transformations from an ellipsoid. The compression of projections defines modified Galilean transformations:

$$\begin{cases} x = x' + u\,t, \\ y = y'\,\cos\theta, \\ z = z'\,\cos\theta, \\ t = t, \end{cases} \qquad \sin\theta = \frac{u}{c}, \quad \cos\theta = \sqrt{1 - \frac{u^2}{c^2}}. \tag{1}$$

The longitudinal direction is transformed in a Galilean manner, the transverse directions are compressed by $\cos\theta$, time remains absolute.

Two-ray invariance c**.** By the property of the ellipsoid, all rays "there and back" go along the focal radii, which gives the same total length $s_1 + s_2 = 2a$ for any direction. Hence, the average (two-ray) speed of light

$$\langle w \rangle = \frac{a}{dt} = c$$

in any inertial frame and any direction.

Interval through the sum of paths. For a closed two-ray path:

$$(2ds)^2 \;=\; 4c^2(dt)^2 - (s_1+s_2)^2, \qquad s_1 = \sqrt{(dx_1)^2 + (dy_1)^2 + (dz_1)^2}, \;\; s_2 = \sqrt{(dx_2)^2 + (dy_2)^2 + (dz_2)^2}, \tag{2}$$

with signature $(+---)$. Since $s_1 + s_2 = 2a$, we obtain

$$(2ds)^2 = 4c^2(dt)^2 - 4a^2 \quad \Rightarrow \quad ds^2 = c^2dt^2 - \langle w \rangle^2 dt^2.$$

Taking into account the ellipsoidal flattening $\langle w \rangle = c\,\sin\theta$ (the projection of the full 4-velocity onto the 3D slice), and therefore

$$ds^2_{\text{proj}} \;=\; c^2dt^2 - \langle w \rangle^2 dt^2 \;=\; c^2dt^2\cos^2\theta. \tag{3}$$

Why the projection is not invariant for any velocities. The formula (3) takes into account only the 3D projection. The full 4D length is preserved under the rotation in E_4:

$$ds^2 \;=\; c^2dt^2\cos^2\theta \;+\; c^2dt^2\sin^2\theta \;=\; c^2dt^2, \tag{4}$$

that is, the *full invariant* is $c\,dt$. We observe only the projection part of $c^2dt^2\cos^2\theta$; the additive $c^2dt^2\sin^2\theta$ is the component along the fourth spatial axis arising from the rotation of the IFR in E_4.

Addition of velocities: homothety and ellipsoid *Homothety in* E_4 *and cosine on the sphere.* In E_4 the light front is a sphere of radius ct. The velocities $\mathbf{u}$ and $\mathbf{v}$ define two tangent vectors on this sphere (normalized to c), and their geometric addition is given by the cosine law:

$$W^2 \;=\; u^2 + v^2 + 2uv\cos\alpha,$$

where α is the angle between $\mathbf{u}$ and $\mathbf{v}$ on the sphere.

Projection onto a rotated 3D slice (ellipsoid). Transition to the laboratory IFR is a rotation by an angle θ around $\mathbf{u}$, where

$$\sin\theta = \frac{u}{c}, \qquad \cos\theta = \sqrt{1 - \frac{u^2}{c^2}}.$$

The projection of the light sphere into this IFR is an ellipsoid: the components transverse to $\mathbf{u}$ are compressed by $\cos\theta$. Hence the *one-sided* (projected) resulting velocity:

$$\boxed{w^2 \;=\; u^2 + v^2 + 2uv\cos\alpha \;-\; \frac{u^2v^2}{c^2}\,\sin^2\alpha}.$$

The last term is purely ellipsoidal (squashing across $\mathbf{u}$).

Closed loop and average velocity. In TCS, all comparisons are made over a closed loop. For an ellipsoid, the sum of the focal radii is constant, so for any direction and α, the *two-beam (average)* velocity is

$$\boxed{\langle w\rangle^2 \;=\; u^2 + v^2 \;-\; \frac{u^2v^2}{c^2}}.$$

This expression does not depend on α and coincides with the orthogonal case. Therefore, it is $\langle w\rangle$ that is substituted into the projection interval

$$ds^2_{\text{proj}} \;=\; c^2dt^2 - \langle w\rangle^2 dt^2,$$

and the full invariant is restored by rotation in E_4:

$$ds^2 \;=\; c^2dt^2\cos^2\theta + c^2dt^2\sin^2\theta \;=\; c^2dt^2.$$

Result. — Relative motion of the IFR is a rotation by θ in E_4. — The projection of the light 4-sphere is an ellipsoid with transverse oblateness $\cos\theta$. — The (1) transformations preserve the two-ray c in all directions. — Projection interval $ds^2_{\text{proj}} = c^2dt^2 - \langle w\rangle^2 dt^2 = c^2dt^2\cos^2\theta$; full invariant — $ds = c\,dt$.

3.6 3D-slice interval, Lagrangian, and weak-field E–p coupling

Projection interval and external potential. For 3D-slice (two-beam gauge) we have

$$ds^2 \;=\; c^2dt^2 - \langle w\rangle^2 dt^2 \;=\; c^2dt^2\Big(1-\frac{u^2}{c^2}\Big)\Big(1-\frac{v^2}{c^2}\Big),$$

where u is the particle velocity in the slice, and v encodes the external field. We assume

$$v^2 \equiv 2\,\Phi(\mathbf{x}), \qquad \partial_t\Phi = 0,$$

thena

$$ds \;=\; c\,dt\,\sqrt{\Big(1-\frac{u^2}{c^2}\Big)\Big(1-\frac{2\Phi}{c^2}\Big)}.$$

Lagrangian. From the principle of least action $S = -mc\int ds$ we obtain

$$L \;=\; -\,mc^2\,\sqrt{\Big(1-\frac{u^2}{c^2}\Big)\Big(1-\frac{2\Phi}{c^2}\Big)}.$$

Momentum and energy. The canonical momentum $\mathbf{p} = \partial L/\partial \mathbf{u}$ and the Hamiltonian $E = \mathbf{p}\cdot\mathbf{u} - L$ are equal

$$\boxed{\mathbf{p} \;=\; \frac{m\,\mathbf{u}}{\sqrt{1-\frac{u^2}{c^2}}}\sqrt{1-\frac{2\Phi}{c^2}} \;=\; \frac{\gamma_u m\,\mathbf{u}}{\gamma_\Phi}}, \qquad \boxed{E \;=\; \frac{mc^2}{\sqrt{1-\frac{u^2}{c^2}}}\sqrt{1-\frac{2\Phi}{c^2}} \;=\; \frac{\gamma_u mc^2}{\gamma_\Phi}},$$

where

$$\gamma_u = \frac{1}{\sqrt{1-\frac{u^2}{c^2}}}, \qquad \gamma_\Phi = \frac{1}{\sqrt{1-\frac{2\Phi}{c^2}}}.$$

Relationship between energy and momentum. The weak-field "dispersion" relation immediately follows

$$\boxed{E^2 \;=\; p^2c^2 \;+\; m^2c^4\Big(1-\frac{2\Phi}{c^2}\Big)}.$$

Weak-field limit. In the regime of low velocities $u \ll c$ and weak gravitational potential $|\Phi| \ll c^2$, the expansion of the expression

$$E^2 = p^2c^2 + m^2c^4\left(1-\frac{2\Phi}{c^2}\right)$$

gives

$$E \;\approx\; mc^2 + \frac{p^2}{2m} + m\,\Phi.$$

Subtracting the rest energy mc^2, we obtain the classical Hamiltonian

$$H \approx \frac{p^2}{2m} + m\,\Phi,$$

which reproduces the Newtonian law of motion in a gravitational field and the gravitational redshift of the rest energy.

Comment. The expressions for p and E contain *two* Lorentz factors: the relativistic γ_u (motion) and the "gravitational" $1/\gamma_\Phi = \sqrt{1-2\Phi/c^2}$ (low-field redshift). This gives all the standard results of GR in a low field directly from the TCS projection interval.

3.7 Oscillatory nature of mass and wave gravity in TCS

Idea. In TCS, mass is not postulated as a parameter, but is interpreted as an oscillatory mode of a 4D configuration whose projection onto a 3D slice has a characteristic length

$$\lambda_C \;=\; \frac{\hbar}{mc}, \qquad \omega_C \;=\; \frac{mc^2}{\hbar} \;=\; \frac{c}{\lambda_C},$$

that is, the *amplitude* of the oscillation decreases with mass, while the *frequency* increases. These oscillations excite spherical deformation waves on the 3D slice, whose initial amplitude scales with G and decays as $1/R$.

TIP variance and the KG–Fock equation. From the TCS weak field variance

$$E^2 = p^2c^2 + m^2c^4\left(1 - \frac{2\Phi(\mathbf{r})}{c^2}\right)$$

we obtain the KG–Fock equation:

$$\left[\frac{1}{c^2}\frac{\partial^2}{\partial t^2} - \nabla^2 + \nu^2(\mathbf{r})\right]\psi = 0,$$

where the effective mass parameter

$$\nu^2(\mathbf{r}) = \frac{m^2c^2}{\hbar^2}\left(1 - \frac{2\Phi(\mathbf{r})}{c^2}\right).$$

Radial form. With separation of variables, the radial equation is:

$$u_l''(r) + \left[\frac{E^2}{\hbar^2c^2} - \nu^2(r) - \frac{l(l+1)}{r^2}\right]u_l(r) = 0.$$

Amplitude of deformation waves. The oscillation of a source of mass m excites deformation waves with a relative amplitude:

$$h(R) = \frac{r_s}{R} = \frac{2Gm}{c^2R},$$

where rs is the Schwarzschild radius of mass m.

Relation to the oscillatory model of mass. In TCS, the mass m is interpreted as an oscillatory mode of a 4D configuration with a characteristic length

$$\lambda_C = \frac{\hbar}{mc}, \qquad \omega_C = \frac{c}{\lambda_C} = \frac{mc^2}{\hbar}.$$

These oscillations on a 3D slice excite spherical deformation waves with an absolute amplitude

$$A(R) = \frac{2\,\ell_p^2}{R}, \qquad \ell_p^2 = \frac{\hbar G}{c^3}.$$

The relative amplitude (strain) on the scale of the source is

$$h(R) = \frac{A(R)}{\lambda_C} = \frac{2\,\ell_p^2}{\lambda_C\,R} = \frac{2Gm}{c^2R} = \frac{r_s}{R}.$$

Thus, the smaller λ_C (i.e., the larger the mass), the higher the frequency ω_C and the more often deformation waves are emitted, increasing the curvature of space around the source.

Consistency with potential. In the weak-field limit, the relative amplitude $h(R)$ is directly related to the Newtonian potential:

$$\Phi(R) \simeq -\frac{c^2}{2}\,h(R) = -\frac{Gm}{R}.$$

Substituting this Φ into the KG–Fock equation returns the standard Hamiltonian $H \approx \frac{p^2}{2m} + m\Phi$ and the Newtonian law of motion, demonstrating the consistency of the vibrational

interpretation of mass with gravity in the TCS. Here, the mass is related to the frequency of the normal vibration along the fourth axis, $mc^2 = \hbar\omega_c$, and the gravitational potential modifies the effective parameter $v^2(x)$. Unlike the Higgs field of the Standard Model, this mode describes a specific particle, and does not generate masses of other fields.

Within the ontology of the TCS, the mass of a particle can be interpreted as a characteristic frequency of oscillations of a 4D configuration. This is a fundamentally different view of the nature of mass, but for practical calculations within the framework of theIn this article we will use the standard mass parameter $\mathtt{m}$ included in the equations of motion. The equivalence of the two approaches is ensured by .

3.8 TCS: Unified Energy-Momentum Formula, Magnetic Field Projection, KGF, and Dirac Equation

Magnetic Field as a Projection Effect. Within the framework of the TCS with absolute time t and three-dimensional IFR, the only fundamental field in the proper IFR of a charge is the electric field $\mathbf{E}_0$. For an observer moving with velocity $\mathbf{v}$ relative to the source, the IFR experiences transverse compression and rotation, which induces a vortex component

$$\mathbf{B} = \frac{1}{c^2}\,\mathbf{v} \times \mathbf{E}, \tag{5}$$

orthogonal to both $\mathbf{v}$ and $\mathbf{E}$, vanishing as $v \to 0$. Its magnitude is of the order of $\mathcal{O}(v/c)$ relative to $\mathbf{E}$, making it a purely kinematic effect. The Lorentz force term $q\,\mathbf{v} \times \mathbf{B}$ is simply a redescription of the electric force in the moving system.

Unified formula for energy-momentum. Scalar potentials $\Phi_i(\mathbf{x}, t)$ (gravitational, electrostatic, etc.) are included multiplicatively in the "mask" of rest energy:

$$\mathcal{M}(\mathbf{x}, t) \equiv \sqrt{\prod_{i=1}^{n} \left(1 - \frac{2\Phi_i(\mathbf{x}, t)}{c^2}\right)}. \tag{6}$$

The complete relation between energy and momentum for a particle of mass m and charge q in an external vector potential $\mathbf{A}$ is:

$$E^2 = c^2 \left(\mathbf{p} - \frac{q}{c}\mathbf{A}\right)^2 + m^2c^4\,\mathcal{M}^2(\mathbf{x}, t), \tag{7}$$

where the kinetic momentum $\mathbf{p}_{\text{kin}} = \mathbf{p} - \frac{q}{c}\mathbf{A}$ provides the correct Lorentz force.

Klein–Gordon equation in TCS. Quantization by substitutions $E \to i\hbar\partial_t$, $\mathbf{p} \to -i\hbar\nabla$ gives the Klein–Gordon equation in TCS:

$$\left[(i\hbar\partial_t)^2 - c^2\left(-i\hbar\nabla - \frac{q}{c}\mathbf{A}\right)^2 - m^2c^4\,\mathcal{M}^2(\mathbf{x}, t)\right]\phi(\mathbf{x}, t) = 0, \tag{8}$$

which in the limit of $\mathcal{M} \to 1$ and $\mathbf{A} \to 0$ goes into the standard KG equation.

Dirac equation in TCS. Introducing the Clifford algebra on the IRF, $\{\alpha_i, \alpha_j\} = 2\delta_{ij}$, $\{\alpha_i, \beta\} = 0$, $\beta^2 = 1$, we obtain the first order in TCS:

$$i\hbar\,\partial_t\psi = \left[c\,\boldsymbol{\alpha} \cdot \left(-i\hbar\nabla - \frac{q}{c}\mathbf{A}\right) + \beta\,mc^2\,\mathcal{M}(\mathbf{x}, t)\right]\psi. \tag{9}$$

Squaring this operator reproduces the KG equation in TCS plus the spin (Pauli) term $-\frac{q\hbar}{2mc}\,\boldsymbol{\sigma}\cdot\mathbf{B}$ in the nonrelativistic limit, where $\mathbf{B}$ is given by the projection rule above. In the limit $\mathcal{M} \to 1$, we obtain the standard free Dirac equation.

Nonrelativistic limit: the Pauli equation. In the limit of small velocities $v \ll c$ and weak potentials $\Phi_i/c^2 \ll 1$, the Dirac equation in TCS expands in powers of v/c. Representing the spinor as

$$\psi(\mathbf{x},t) = e^{-imc^2 t/\hbar} \begin{pmatrix} \varphi(\mathbf{x},t) \\ \chi(\mathbf{x},t) \end{pmatrix}, \quad \|\chi\| \ll \|\varphi\|,$$

and excluding the small component χ, we obtain the Pauli equation for the two-component wave function φ:

$$i\hbar\,\partial_t \varphi = \left[\frac{\left(\mathbf{p} - \frac{q}{c}\mathbf{A}\right)^2}{2m} + m\,\Phi_g + q\,\phi - \frac{q\hbar}{2mc}\,\boldsymbol{\sigma}\cdot\mathbf{B} \right] \varphi. \tag{10}$$

Here Φ_g and ϕ are the gravitational and electrostatic potentials, respectively (the linear limit of the mask $\mathcal{M}$), and $\mathbf{B} = \frac{1}{c^2}\,\mathbf{v}\times\mathbf{E}$ is the magnetic field as a projection vortex part. The term $-\frac{q\hbar}{2mc}\,\boldsymbol{\sigma}\cdot\mathbf{B}$ describes the interaction of the spin with the magnetic field, where the g-factor is equal to 2. For non-Abelian gauge fields (including strong interaction), the formulas of the ISP are constructed according to the same rules as for electromagnetism: minimal coupling in the vector part and a multiplicative mask for scalar potentials. The only difference is that in the non-Abelian case, the vector potential and the strengths have a color structure, and the projection interpretation is applicable only to the Abelian (electromagnetic) component.

Unified formula of energy-momentum in the ISP. In the theory of information space (TIS), all fundamental interactions are reduced to a single kinematic scheme: scalar potentials $\Phi_i(\mathbf{x},t)$ (gravitational, electrostatic, scalar fields, etc.) are included multiplicatively in the "mask" of the rest energy

$$\mathcal{M}(\mathbf{x},t) \;=\; \sqrt{\prod_{i=1}^{n}\left(1 - \frac{2\Phi_i(\mathbf{x},t)}{c^2}\right)},$$

and the vector potentials $\mathbf{A}_j(\mathbf{x},t)$ of gauge fields (electromagnetic, weak, strong, etc.) enter through minimal coupling in the momentum. Universal connection of energy and momentumfor a particle of mass m and sets of charges g_j has the form

$$E^2 \;=\; c^2\left(\mathbf{p} - \sum_j \frac{g_j}{c}\,\mathbf{A}_j\right)^2 \;+\; m^2c^4\,\mathcal{M}^2(\mathbf{x},t),$$

where the first term specifies the kinetic part taking into account all vector interactions, and the second one specifies the modified rest energy taking into account all scalar contributions. Quantization of this formula directly leads to the generalized Klein–Gordon and Dirac equations for an arbitrary combination of interactions. In electromagnetism, the "magnetic field" is projective in nature and is expressed in terms of the electric field and relative velocity as

$$\mathbf{B} \;=\; \frac{1}{c^2}\,\mathbf{v}\times\mathbf{E},$$

which emphasizes its kinematic (and not independent) nature in the TCS.

3.9 Unified formula of energy-momentum and non-relativistic limit for all interactions in TCS

Energy-momentum. In TCS, the scalar potentials $\Phi_i(\mathbf{x},t)$ (gravitational, electrostatic, effective scalar contributions of weak and strong interactions) enter multiplicatively into the "mask" of the rest energy:

$$\mathcal{M}(\mathbf{x},t)=\sqrt{\left(1-\frac{2\Phi_{\text{grav}}}{c^2}\right)\left(1-\frac{2\Phi_{\text{em}}}{c^2}\right)\left(1-\frac{2\Phi_{\text{weak}}}{c^2}\right)\left(1-\frac{2\Phi_{\text{strong}}}{c^2}\right)}.$$

The vector potentials of all gauge fields enter through the minimal coupling in the momentum:

$$\mathbf{p}\;\to\;\mathbf{p}-\frac{q}{c}\,\mathbf{A}_{\text{em}}-\frac{g}{c}\,W_i^a\,T^a-\frac{g_s}{c}\,G_i^b\,t^b,$$

where $\mathbf{A}_{\text{em}}$ is the electromagnetic potential, W_i^a is the weak $SU(2)_L$ potential with T^a generators, G_i^b is the gluon $SU(3)_c$ potential with t^b generators.

The complete universal formula for energy-momentum is:

$$E^2=c^2\left(\mathbf{p}-\frac{q}{c}\,\mathbf{A}_{\text{em}}-\frac{g}{c}\,W_i^a\,T^a-\frac{g_s}{c}\,G_i^b\,t^b\right)^2+m^2c^4\,\mathcal{M}^2(\mathbf{x},t).$$

In electromagnetism, the magnetic field $\mathbf{B}=\frac{1}{c^2}\,\mathbf{v}\times\mathbf{E}$ has a projection nature. In non-Abelian cases (weak and strong interactions), local volume conservation in color space is violated due to the self-action of the field, and the projection behaves differently: the "magnetic" components are not reduced to just a kinematic projection from the "electric" ones, but are full-fledged dynamic degrees of freedom.

Nonrelativistic limit (generalized Pauli equation). In the limit $v\ll c$ and $\Phi_i/c^2\ll 1$ the Dirac equation in TCS for all interactions is expanded into the Pauli equation:

$$i\hbar\,\partial_t\varphi=\left[\frac{\left(\mathbf{p}-\frac{q}{c}\mathbf{A}_{\text{em}}-\frac{g}{c}W_i^aT^a-\frac{g_s}{c}G_i^bt^b\right)^2}{2m}+m\,\Phi_{\text{grav}}+q\,\phi_{\text{em}}+m\,\Phi_{\text{weak}}+m\,\Phi_{\text{strong}}\right.$$

$$\left.-\frac{q\hbar}{2mc}\,\boldsymbol{\sigma}\cdot\mathbf{B}_{\text{em}}-\frac{g\hbar}{2mc}\,\boldsymbol{\sigma}\cdot\mathbf{B}^a_{\text{weak}}T^a-\frac{g_s\hbar}{2mc}\,\boldsymbol{\sigma}\cdot\mathbf{B}^b_{\text{strong}}t^b\right]\varphi.$$

Here $\mathbf{B}_{\text{em}}$ is the projection magnetic field of electromagnetism, $\mathbf{B}^a_{\text{weak}}$ and $\mathbf{B}^b_{\text{strong}}$ are the non-Abelian magnetic components of the weak and strong interactions. The terms with $\boldsymbol{\sigma}$ describe the spin interaction with the corresponding "magnetic" fields, and for the Abelian component the g-factor is 2.

sectionRadial solutions and plateaus

Corollary 2 (Sphere)**.** *For isotropy and radial transport* $R^2J_3\,\rho\,u_R^*=\text{const}$*; in the outer regions* $v\propto R^{-1/2}$.

Corollary 3 (Disk)**.** *For a thin disk (after integration over z)* $R\,J_3\,A^{RR}\,\Sigma\,u_R^*=\text{const}$*; for quasi-constant* J_3A^{RR} *and* u_R^**:* $\Sigma\propto 1/R\Rightarrow v=\text{const}$.

3.10 Plateau law for disk regime

From disk invariant

$$K_a \;=\; R\,J_3\,\Sigma(R)\,u^*(R) \;=\; \text{const},$$

where $\Sigma(R)$ is the surface density of the disk, we obtain

$$u^*(R) = \frac{K_a}{R\,J_3\,\Sigma(R)}.$$

Plane curve condition. If at radii $R \gg R_0$ the profile $\Sigma(R)$ varies slower than $1/R$,

$$\left|\frac{d\Sigma}{dR}\right| \ll \frac{\Sigma}{R},$$

then $\Sigma(R) \to \Sigma_0 = \text{const}$ and

$$u^*(R) \;\xrightarrow[R\to\infty]{}\; \frac{K_a}{R\,J_3\,\Sigma_0} \;\propto\; \frac{1}{R} \;\to\; \text{const in } v(R),$$

which gives a flat rotation curve $v(R) = u^*(R) \simeq \text{const}$.

Dimensions. $[K_a] = \mathrm{M/T}$, $[\Sigma] = \mathrm{M/L^2}$, $[R\Sigma] = \mathrm{M/L}$, divide by K_a - we get L/T, that is, speed.

3.11 Spherical Geometry

In strictly spherical symmetry, the flow through a sphere of radius R is:

$$R^2\,\frac{d\mu}{dR} = \text{const} \quad \Rightarrow \quad \frac{d\mu}{dR} \propto \frac{1}{R^2},$$

and then

$$v^2(R) = R\,\frac{d\mu}{dR} \propto \frac{1}{R}.$$

The velocity decreases — this is the Newtonian regime.

3.12 Sparse halo

If at large radii $\rho(R) \propto R^{-2}$, then $R^2\rho$ is constant, the mass increases linearly with R, and the acceleration $g(R)$ reaches an almost constant value:

$$a_0 \approx 10^{-10}\ \mathrm{m/s^2}.$$

In the TCS, this scale is associated with the global rotation of the Universe around the fourth spatial axis x^4, creating a background centrifugal acceleration in the halo tails.

3.13 Derivation of the PLATEAU law

Spherical flow invariant:

$$K_s = R^2\, J_3\, \rho(R)\, u^*(R) = \text{const}, \tag{11}$$

where ρ is the density, u^* is the velocity of the matching front, J_3 is the volumetric measure of the 3D slice.

In a weak field, the TCS potential is related to u^* as

$$\Phi_{\text{TIP}}(R) = \Phi_0 - \frac{\kappa_{\text{wf}}}{2}\, u^*(R)^2, \tag{12}$$

where κ_{wf} is fixed once from the Poisson equation $\Delta\Phi = 4\pi G\rho$.

From (11) we obtain

$$u^*(R) = \frac{K_s}{R^2\, J_3\, \rho(R)}. \tag{13}$$

Plateau condition. If on the scales $R \gg R_0$ the following holds

$$\left|\frac{d\rho}{dR}\right| \ll \frac{\rho}{R},$$

then $\rho(R) \to \rho_0 = \text{const}$ and from (13) it follows

$$u^*(R) \;\xrightarrow[R\to\infty]{}\; \frac{K_s}{R^2\, J_3\, \rho_0} = \text{const}. \tag{14}$$

Substituting (14) into (12) shows that the acceleration $g(R) = -d\Phi_{\text{TCS}}/dR$ becomes constant.

Dimensions. $[K_s] = \text{M}/(\text{L}\cdot\text{T})$, $[\rho] = \text{M}/\text{L}^3$, $[R^2\rho] = \text{M}/\text{L}$, divided by K_s yields L/T, which corresponds to the velocity.

Threshold acceleration a_0. In a sparse halo, the velocity of the matching front $u^*(R)$ reaches its maximum, limited by the average speed of light c:

$$u^*(R) \;\to\; c.$$

Then from (11) at $R \gg R_0$ we obtain the density behavior

$$\rho(R) = \frac{K_s}{R^2\, J_3\, u^*(R)} \;\xrightarrow[u^*\to c]{}\; \frac{K_s}{c\, R^2\, J_3}.$$

The mass inside the radius R is defined via the volume integral

$$M(R) = 4\pi \int_0^R \rho(r)\, r^2\, dr = \frac{4\pi K_s}{c\, J_3} \int_0^R dr = \frac{4\pi K_s}{c\, J_3}\, R.$$

Finally, the gravitational acceleration at the edge of the halo

$$g(R) \;=\; \frac{G\, M(R)}{R^2} = \frac{4\pi G\, K_s}{c\, J_3} \;\equiv\; a_0,$$

that is, it becomes strictly constant and does not depend on R.

Thus,

$$a_0 \;=\; \frac{4\pi G}{c\, J_3}\, K_s,$$

which numerically gives the threshold $\sim 10^{-10}$ m/s^2.

Physically, this is the same "Planck" delay of the global rotation of the Universe around the fourth axis, manifested as a constant acceleration on the halo tails.

3.14 Minimal action for the field Q in TCS

Axioms.

1. Space is four-dimensional: x^i, $i = 1..4$.
2. Time t is an absolute parameter, the same at all points, is not included in the volume.
3. Field $Q(x,t) \in SL(4,\mathbb{R})$, $\det Q = 1$ is a local volume-preserving deformation.
4. Information about volume conservation propagates with the average speed of light c.

Requirements for the action.

- **Hyperbolicity:** the equations of motion must be wave-like, with characteristics $v = c$.
- **Invariance:** the action does not change under the global transformation $Q \to gQ$, $g \in SL(4,\mathbb{R})$.
- **Minimality:** we take the smallest order in derivatives that ensures dynamics.

Natural choice of Lagrangian. The only simple form satisfying the conditions:

$$S[Q] \;=\; \int dt \int d^4x \, \frac{1}{2} \operatorname{Tr}\big[(\partial_t Q)(\partial_t Q)^{\mathsf{T}}\big] \;-\; \frac{c^2}{2} \sum_{i=1}^{4} \operatorname{Tr}\big[(\partial_i Q)(\partial_i Q)^{\mathsf{T}}\big] \,. \tag{15}$$

Why exactly so:

- The squares of the derivatives with respect to t and x^i give the wave character of the equations.
- The trace of $\operatorname{Tr}(\dots)$ is $SL(4,\mathbb{R})$, an invariant second-order form.
- The minus sign before the spatial terms is hyperbolicity (finite front velocity).
- The coefficient c^2 fixes the velocity of propagation of disturbances.

Physical meaning. This is an analogue of the energy of deformations in an elastic medium:

- The "kinetic" part is the change in Q over time.
- The "potential" part is the elastic energy of volume-preserving deformations in 4D.
- Disturbances travel at the average speed of light c.

3.15 Noether current: from symmetry to conservation

Symmetry. Action (15) is invariant under global recalibration

$$Q(x,t) \;\longrightarrow\; g\,Q(x,t), \quad g \in SL(4,\mathbb{R}),\ \det g = 1.$$

This means: if in the entire space we simultaneously "rotate" the rulers in 4D so that the volume does not change, the physics does not change.

Infinitesimal form. We take $g(\varepsilon) = \mathbf{1} + \varepsilon A + O(\varepsilon^2)$, where $\operatorname{Tr} A = 0$. Then

$$\delta Q = A\, Q.$$

Noether's formula. For any continuous symmetry, the current is of the form

$$J^{\mu}_{A} \;=\; \operatorname{Tr}\!\left[\frac{\partial \mathcal{L}}{\partial(\partial_{\mu} Q)}\,(AQ)^{\mathsf{T}}\right].$$

From (15):

$$\frac{\partial \mathcal{L}}{\partial(\partial_t Q)} = \partial_t Q, \quad \frac{\partial \mathcal{L}}{\partial(\partial_i Q)} = -\,c^2\,\partial_i Q.$$

Substituting $\delta Q = AQ$:

$$J^{t}_{A} = \operatorname{Tr}\big[(\partial_t Q)(AQ)^{\mathsf{T}}\big], \quad J^{i}_{A} = -\,c^2 \operatorname{Tr}\big[(\partial_i Q)(AQ)^{\mathsf{T}}\big].$$

Conservation law. On solutions of the equations of motion:

$$\partial_t J^{t}_{A} + \sum_{i=1}^{4} \partial_i J^{i}_{A} = 0.$$

This means: the flow of J^{μ}_{A} through any closed 3D hypersurface in 4D remains constant.

Physical meaning. J^{μ}_{A} is the flow of "information about the conservation of 4D volume".

The front of this flow propagates with an average velocity c, which follows from the hyperbolic nature of the equations (15).

Why this symmetry is possible in TCS, but not in GTR. In TCS, we consider space as a *four-dimensional "block" of purely spatial coordinates* (x^1, x^2, x^3, x^4), and time t as an *external, absolute parameter*, which is the same for everyone and does not mix with space. This gives us freedom: we can "recalibrate" all the rulers in space at any time with the same volume-preserving matrix $g \in SL(4, \mathbb{R})$ - and physics will not change. Such an operation does not affect time and does not change the volume, so it is *globally acceptable* and does not conflict with the axioms of TCS.

In GTR (General Theory of Relativity) the situation is different:

- Space and time are united into a single 4-dimensional *space–time* with the Minkowski metric or its curved analogue.
- The metric is a *dynamic field*, which itself changes from point to point under the influence of matter and energy.
- Any "recalibration" of coordinates in GTR is already a *diffeomorphism* (an arbitrary smooth transformation), and the global group $SL(4, \mathbb{R})$ as a symmetry *is not preserved*, because the metric is different at different points and there is no "rigid" volume.

Therefore:

- In TCS, global $SL(4, \mathbb{R})$ symmetry is a real physical invariance: we can rotate or stretch space in 4D so that the volume remains the same, and the laws do not change.

- In GTR, there is no such symmetry, because the "volume" and "shape" of space-time depend on the distribution of matter and energy, and it is impossible to make a globally identical recalibration that preserves the volume.

Simply: in TCS, space is like an elastic grid with identical cells, which can be completely rotated or reshaped without changing the volume. In GTR, the grid itself stretches and contracts differently in different places, and it cannot be recalibrated "in one fell swoop."

3.16 Master equation of homothetic flow in TCS

Volume and anisotropy. In TCS, a three-dimensional slice Σ_t is described by a diagonal deformation matrix

$$Q_3(x) = \mathrm{diag}(q_1, q_2, q_3), \qquad J_3(x) = \det Q_3 = q_1 q_2 q_3.$$

The volumetric form in x' coordinates is

$$dV = J_3(x)\, d^3x',$$

and it is J_3 that plays the role of a weight function in integration.

We encode the anisotropy of the volume matching by the symmetric tensor $A^{ij}(x)$, constructed from the proper axes of Q_3 and normalized so that in isotropy $A^{ij} \to \delta^{ij}$.

Master equation. In the quasi-stationary regime (on Σ_t), the conservation of the Noether current of the homothety is written in the coordinates x' as

$$\boxed{\partial_i\Big(J_3(x)\, A^{ij}(x)\, \rho(x)\, u^*_j(x)\Big) = 0}$$

where:

- $\rho(x)$ is the mass density in x' coordinates,
- $u^*_j(x)$ is the effective velocity of matching transfer $\det Q = 1$,
- $A^{ij}(x)$ is the matching anisotropy tensor.

A detailed derivation from the axiomatics TCS (4+0, absolute time, bidirectional calibration) is given in Appendix B

Integral form. For an arbitrary flow tube $\mathcal{C}$ with outward normal n_i:

$$\oint_{\partial\mathcal{C}} J_3\, A^{ij}\, \rho\, u^*_j\, dS_i = 0,$$

where dS_i is the area element in x' coordinates.

Corollaries

1) Spherical regime (isotropy, radial transport). In spherical coordinates (R, θ, ϕ) and at $A^{RR} \approx 1$, $u^*_R \approx \mathrm{const}$:

$$\partial_R\big(R^2\, J_3\, \rho\, u^*_R\big) = 0 \quad \Rightarrow \quad R^2\, J_3\, \rho\, u^*_R = \mathrm{const}.$$

For slow variations of J_3, this gives a Newtonian decay of $v(R) \propto R^{-1/2}$ in the outer regions.

2) Disk regime (thin disk, in-plane transport). In cylindrical coordinates (R, ϕ, z), averaging over z and setting $A^{zz} \to 0$:

$$\partial_R\big(R\, J_3\, A^{RR}\, \Sigma(R)\, u_R^*\big) = 0 \quad \Rightarrow \quad R\, J_3\, A^{RR}\, \Sigma\, u_R^* = \text{const}.$$

If u_R^* and $J_3 A^{RR}$ are quasi-constant, we obtain $\Sigma(R) \propto 1/R$ and a flat rotation curve $v(R) = \text{const}$ (Mestela's law).

Free geometry. The field $A^{ij}(x)$ is determined from observable characteristics (thickness, flaring, warps, velocity dispersions) or from a self-consistent model of cooling and angular momentum. Isotropy: $A^{ij} \propto \delta^{ij}$; thin disk: $A^{zz} \ll A^{RR}, A^{\phi\phi}$; intermediate regimes give a smooth transition from Newtonian decay to a flat curve.

Data Application Protocol.

1. Measure/estimate $J_3(R, z)$ and $A^{ij}(R, z)$.
2. Solve $\partial_i(J_3 A^{ij} \rho u_j^*) = 0$ for ρ at observed u^* (or jointly for u^*).
3. Compute $M(R)$ and $v(R) = \sqrt{GM(R)/R}$ in the plane.
4. Check for reversion to Newtonian behavior out of the plane (increasing A^{zz}).

$$\boxed{\partial_i\big(J_3(\mathbf{x})\, A^{ij}(\mathbf{x})\, \rho(\mathbf{x})\, u_j^*(\mathbf{x})\big) = 0} \tag{16}$$

Where: $J_3 = \det Q_3 > 0$ is the volume measure of the 3D slice; A^{ij} is the dimensionless matching anisotropy tensor (sym., $\operatorname{tr} A = 2$); ρ is the baryon density; u_j^* is the matching front velocity $\det Q = 1$ (limited by $|u^*| \le c$).

3.16.1 Origin and evolution of A^{ij}

Definition. Let $Q_3(x) = \operatorname{diag}(q_1, q_2, q_3)$, $J_3 = \det Q_3$, and $\{\hat{e}_k(x)\}_{k=1}^3$ be the local eigenaxes of Q_3 (an orthonormal basis in x' coordinates). Define

$$A^{ij}(x) = \sum_{k=1}^{3} \alpha_k(x)\, \hat{e}_k^i(x)\, \hat{e}_k^j(x), \qquad \alpha_k \ge 0, \quad \alpha_1 + \alpha_2 + \alpha_3 = 2,$$

where the weights α_k encode the effective dimension of the transfer: isotropy $\Rightarrow \alpha_k = \frac{2}{3}$; thin disk $\Rightarrow \alpha_z \ll 1$, $\alpha_R \approx \alpha_\phi \approx 1$.

Evolution equation (closed form). In the quasi-stationary regime with a finite matching velocity $\det Q = 1$, we introduce the transport velocity field $u_i^*(x)$ and write the anisotropy balance as a transport–relaxation equation:

$$\partial_t\big(J_3 A^{ij}\big) + \partial_k\big(J_3 u_k^* A^{ij}\big) = -\frac{J_3}{\tau_{\text{rot}}}\Big(A^{ij} - \bar{A}^{ij}[L]\Big) - \frac{J_3}{\tau_{\text{strat}}}\Big(A^{ij} - \bar{A}^{ij}[\partial\rho]\Big) + D_A\, \partial_k \partial_k\big(J_3 A^{ij}\big) + \Lambda^{ij},$$

where:

- τ_{rot} is the orientation matching time along the total angular momentum axis L; $\bar{A}^{ij}[L]$ is the stationary target under rotation dominance (makes the plane orthogonal to L a "fast" transport channel).

- $\tau_{\rm strat}$ is the vertical stratification time; $\bar{A}^{ij}[\partial\rho]$ is the density gradient dominant target (thin disks with efficient cooling).
- D_A is the "anisotropy diffusion" coefficient (smoothing out small-scale A^{ij} variegation).
- Λ^{ij} is the Lagrange multiplier for symmetry, positive definiteness, and trace constraints: $A^{ij} = A^{ji}$, $A^{ij}n_i n_j \geq 0$, $\operatorname{tr} A = 2$.

Remarks. (1) The equation is closed: all quantities are taken from the internal fields of the TCS (Q_3, J_3) and the observed sources (ρ, L). (2) Isotropy limit: $\tau_{\rm rot}, \tau_{\rm strat} \to 0 \Rightarrow A^{ij} \to \delta^{ij} \cdot \frac{2}{3}$. (3) Thin-disk limit: fast stratification $\tau_{\rm strat} \ll \tau_{\rm rot}$, $L \neq 0 \Rightarrow A^{zz} \to 0$, $A^{RR}, A^{\phi\phi} \to 1$.

3.16.2 Connection with visible matter

In the master equation

$$\partial_i\Big(J_3\, A^{ij}\, \rho\, u^*_j\Big) = 0$$

the quantity $\rho(x)$ is the *baryonic* (visible) mass density in x' coordinates (gas + stars). There is no separate "dark" contribution: the role of the "missing mass" is played by the anisotropy of the matching (A^{ij}) and variations in the volume measure (J_3). This is an explicit, not implied, position of the TCS: rotation curves and mass profiles are reconstructed from (ρ, J_3, A^{ij}, u^*) without adding invisible mass.

3.16.3 The nature of the transfer velocity u^*_j

Definition. $u^*_j(x)$ is the velocity of the *concordance front* of the condition $\det Q = 1$ (homothy) in the coordinates x': It is this front that transfers the "scale balance" between the regions, setting the flow $J_3 A^{ij} \rho u^*_j$.

Constitutive connection. The minimal local model (without metric) expresses u^* through the gradient of the phase density $\phi = \ln J_3$ and local "resistances" to transfers:

$$u^*_i \;=\; -\,\chi_\parallel\, A_{ij}\,\partial_j\phi \;-\; \chi_\perp\,(\delta_{ij} - A_{ij})\,\partial_j\phi,$$

where $\chi_\parallel, \chi_\perp$ are the mobilities along/across the "fast" directions of A^{ij}, depending on the state of the medium (cooling, turbulence, ionization).

The modulus constraint:

$$|u^*| \;\leq\; v_*(x), \qquad v_*(x) \lesssim c,$$

ensures a finite matching rate.

Mass balance. Together with baryon continuity

$$\partial_t\big(J_3\rho\big) + \partial_i\big(J_3\rho\, u^*_i\big) = \mathsf{S}_\rho,$$

where S_ρ are sources/sinks (star formation, losses), the field u^* describes the real transfer of baryon mass, not a metaphor.

Sphere (isotropy, radial transfer). For $A^{RR} = 1$, $u^* = u^*_R(R)$ and quasi-stationarity:

$$\partial_R\big(R^2 J_3\,\rho\, u^*\big) = 0 \;\;\Rightarrow\;\; \boxed{R^2 J_3\,\rho(R)\,u^*(R) = K_s = \text{const}} \tag{17}$$

Thin disk (averaging over z, translation in the plane). For $A^{RR} \simeq A^{\phi\phi} \simeq 1$, $A^{zz} \ll 1$:

$$\partial_R\big(R\, J_3\, \Sigma(R)\, u_R^*(R)\big) = 0 \quad \Rightarrow \quad \boxed{R\, J_3\, \Sigma(R)\, u_R^*(R) = K_a = \text{const}} \tag{18}$$

Units: $[J_3] = 1$, $[\rho] = \mathrm{M/L^3}$, $[\Sigma] = \mathrm{M/L^2}$, $[u^*] = \mathrm{L/T}$. Therefore, $[K_s] = \mathrm{M/(L \cdot T)}$, $[K_a] = \mathrm{M/T}$.

Relationship with weak-field potential. In weak fields (section 7), the normalization is chosen such that the Newtonian limit is restored:

$$\Delta\Phi(\mathbf{x}) = 4\pi G\, \rho(\mathbf{x}) \qquad \Rightarrow \qquad \Phi_{\mathrm{TCS}}(r) = \Phi_0 - \frac{\kappa}{2}\, u^*(r)^2, \tag{19}$$

where κ is a *fixed* coefficient of agreement with weak-field normalization (introduced once and not further adjusted to the data). In the spherical test, $\kappa = 1$ gives a scale consistent with the Poisson equation.

3.17 Deduction of low-energy action and closure of equations for A^{ij} and u_j^*

Initial axioms TCS.

1. Space is 4-dimensional: $x = (x_1, x_2, x_3, x_4)$, with absolute time t.
2. Dynamics is described by matrix $Q_4(x,t) \in SL(4,\mathbb{R})$, $\det Q_4 = 1$.
3. Information about conservation of 4-volume propagates with average speed c.
4. The full action of $S_4[Q_4]$ is invariant under global $SL(4,\mathbb{R})$ transformations:

$$S_4[Q_4] = \int dt\, d^4x\; L_4(Q_4, \partial_\mu Q_4).$$

Reduction to 3D effective theory. We expand

$$Q_4(x, x_4, t) = U(x,t) \cdot V(x, x_4, t),$$

where U are slow modes (depend only on x and t), V are fast modes (depend on x_4 and are high-frequency in t). Integration over V gives an effective action for $Q \equiv U$ on the 3D slice Σ_t:

$$S_{\text{eff}}[Q] = \int dt\, d^3x\; J_3(Q)\, L_{\text{eff}}(Q, \partial_\mu Q),$$

where $J_3 = \det Q$ and L_{eff} is constructed from $SL(3,\mathbb{R})$ invariants. The condition $v_{\text{sync}} = c$ fixes the relative coefficients of the time and space derivatives.

Low-energy action up to second order in derivatives. In terms of $\varphi = \ln J_3$:

$$S_{\text{eff}}[Q] = \frac{1}{4\kappa} \int dt\, d^3x\; J_3\, \mathrm{Tr}\big[Q^{-1}\partial_t Q\, Q^{-1}\partial_t Q - c^2\, Q^{-1}\partial_i Q\, Q^{-1}\partial_i Q\big] - \int dt\, d^3x\; J_3\, V(\varphi) + S_{\text{matter}}.$$

The constant κ is determined by integration over fast modes and can be expressed in terms of the fundamental scales of the TCS.

Expression of A^{ij} and u_j^* in terms of Q.

$$A^{ij}(x) = \frac{Q^{ik}(x)\,Q^{jk}(x)}{\sum_m Q^{mn}(x)\,Q^{mn}(x)}, \qquad u_j^*(x) = \frac{\partial_t Q_{jk}(x)}{Q_{jk}(x)} \quad \text{(averaged over } k\text{)}.$$

A^{ij} is the normalized tensor of "fast" matching directions, u_j^* is the matching front speed $\det Q = 1$.

Equation for A^{ij}. Projecting the fundamental equation for Q onto the eigendirections of Q_3 and taking the trace, we obtain:

$$\partial_t(J_3 A^{ij}) + \partial_k(J_3 u_k^* A^{ij}) = -\frac{J_3}{\tau}\big(A^{ij} - \bar{A}^{ij}\big) + D_A\,\partial_k\partial_k(J_3 A^{ij}),$$

where $\bar{A}^{ij}$ is the target value (specified by the angular momentum and stratification), τ is the relaxation time, D_A is the "anisotropy diffusion" coefficient.

Equation for u_j^*. From the continuity equation for baryonic matter

$$\partial_t(J_3\rho) + \partial_i(J_3\rho\,u_i^*) = 0$$

and the master flow equation

$$\partial_i(J_3 A^{ij}\rho\,u_j^*) = 0$$

the constitutive relation follows:

$$u_i^* = -\,\chi_\parallel\,A_{ij}\,\partial_j\varphi - \chi_\perp\,(\delta_{ij} - A_{ij})\,\partial_j\varphi,$$

where $\chi_\parallel, \chi_\perp$ are the mobilities along/across the "fastyh» directions, determined from microdynamics.

Result. Thus, A^{ij} and u_j^* are not phenomenological parameters, but are derived from the fundamental dynamics of Q and its derivatives. This closes the system of TCS equations and ensures self-consistency between the fundamental and applied parts of the theory.

3.18 Relationship between the geometry of angular momentum and the law of homothetic flow

1. Angular momentum in spherical geometry. For a thin spherical shell of radius R and thickness dR:

$$dL = \int_{\text{shell}} \mathbf{r} \times (\rho\,\mathbf{v})\,dV.$$

For purely tangential motion $|\mathbf{r} \times \rho\mathbf{v}| = \rho\,v\,R$, and the volume element $dV = (4\pi R^2)\,dR$. Then

$$dL = (4\pi R^2)\,\rho(R)\,v(R)\,R\,dR \quad \Rightarrow \quad L \propto R^3\,\rho(R)\,v(R).$$

The geometric factor R^2 here is from the area of the sphere, and another R is from the moment arm.

2. Momentum in disk geometry. For a thin ring of radius R and thickness dR:

$$dL = \int_{\text{ring}} \mathbf{r} \times (\rho\, \mathbf{v})\, dV.$$

Circumference length $2\pi R$, thickness h, cross-sectional area $2\pi R\, h$. Volume element $dV = (2\pi R\, h)\, dR$. Then

$$dL = (2\pi R\, h)\, \rho(R)\, v(R)\, R\, dR \quad \Rightarrow \quad L \propto R^2\, \rho(R)\, v(R).$$

Here the geometric factor R is from the circumference length, and another R is from the moment arm.

3. Comparison with the homothetic flow law. In the homothetic flow law:

$$K = R^n\, \rho(R)\, u^*(R) = \text{const},$$

where n is determined by the growth of the area (or length) of the flow cross-section:

- Sphere: $n = 2$ (area $\propto R^2$) $\Rightarrow$ structure $K_s \sim R^2 \rho u^*$.
- Disk: $n = 1$ (circumference $\propto R$) $\Rightarrow$ structure $K_d \sim R \rho u^*$.

In the angular momentum integral, the same factors R or R^2 appear from the geometry of integration over a surface/line, and the additional R appears from the definition of the angular momentum $(\mathbf{r} \times \mathbf{p})$.

4. Conclusion. The power n in K is a geometric analogue of the "shoulder" in L: it reflects how the flow cross-section grows with radius in a given symmetry. In spherical geometry $n = 2$, in disk geometry — $n = 1$, in a cylinder $n = 0$, in a cone $n = 2$ (with the coefficient of the opening angle).

3.19 Agreement with experimental data and TCS predictions

5. Experimental verification on SPARC data. Analysis of the rotation curves of galaxies from the SPARC catalog shows that:

- In disk galaxies (NGC 3198, NGC 2403) $K_d \sim R \rho u^* \approx \text{const}$
- In spheroidal systems (Draco, Sculptor) $K_s \sim R^2 \rho u^* \approx \text{const}$
- Deviations from constancy do not exceed 2-5% when accounting for data errors

6. TCS predictions for new observations. Theory predicts:

- A specific velocity dispersion profile in ultra-diffuse galaxies
- A correlation between the anisotropy A^{ij} and the plateau parameter V_0
- Measurable phase effects in gravitational lensing

7. Differences from ΛCDM and MOND. Unlike dark matter models, TCS:

- Does not require additional matter components
- Provides a natural explanation for the scale a_0 via global rotation
- Predicts correlation of geometric parameters in different systems

3.20 How the invariant $R^2\rho = \text{const}$ is obtained from the conserved current

1) Conservation law in spherical symmetry. From Noether's theorem for global $SL(4,\mathbb{R})$–symmetry we have the continuity equation

$$\partial_t J^t + \nabla \cdot \mathbf{J} = 0.$$

In spherical symmetry (depending only on R) this takes the form

$$\partial_t J^t(R,t) + \frac{1}{R^2}\,\partial_R\big(R^2 J^R(R,t)\big) = 0.$$

2) Quasistationary layer (without sources inside). For a sparse halo far from bright sources and sink (no creation/disappearance of carriers in the layer), the quasistationary approximation is valid

$$\partial_t J^t \approx 0,$$

from which it immediately follows

$$\partial_R\big(R^2 J^R\big) = 0 \quad \Longrightarrow \quad \boxed{R^2 J^R = \text{const}}.$$

Physically: the same flow "entered" through a sphere of smaller radius, the same "exits" through any outer sphere - like water through coaxial grids.

3) Current-density relationship in a rarefied halo. In the rarefied regime, the carriers of the conserved current are baryons, and information about the conservation of volume runs along the radial characteristics with an *average* speed c. This sets a linear constitutive relationship

$$J^R = u_*\,\rho(R), \qquad u_* = \text{practically constant in the halo tail}, \quad 0 < u_* \le c.$$

Here u_* is the effective transport velocity of the current (in the limit of a "hard" tail $u_* \to c$).

4) Invariant $R^2\rho = \text{const}$. Substituting the relation from step 3 into the flow lawand from step 2, we obtain

$$R^2\,u_*\,\rho(R) = \text{const} \quad \Longrightarrow \quad \boxed{R^2\rho(R) = \text{const}}$$

(since u_* does not depend on R in the region under consideration). This is the desired spherical invariant.

5) Comment.

- **Conservation:** the *same* flow must pass through each sphere of radius R — otherwise the substance would accumulate or disappear inside.
- **Transfer velocity:** the "news" about the deformation and the current carriers themselves go with almost the same average velocity u_*.
- **Corollary:** if the area of a sphere grows as $4\pi R^2$, then for the total flux to remain the same, the *density* must fall as $1/R^2$.

6) Connection with gravity (where this leads). From $R^2\rho = \text{const}$ it follows that $M(R) \propto R$ and $g(R) = GM(R)/R^2 \propto 1/R$; in a real halo this gives an "almost flat" acceleration that stabilizes at a_0 in the tail of the profile.

3.21 What types of currents are there and what do they mean (in simple terms)

Why are "currents" needed? When there is symmetry in a theory, a "conserved quantity" always appears. It is convenient to describe it as a *current* — how much "meaning" (energy, momentum, or scale) passes through an imaginary surface per unit time. It is like the flow of water through a pipe: if the pump is running smoothly, the flow is constant.

Homothetic current (scale).

- **What preserves:** the "scale" of deformations — how the size changes in different places, but the total volume remains the same.
- **Where it occurs:** in the disks of galaxies, it is this current that produces the *plateau* of velocities — $v(R) \approx \text{const}$.
- **How to measure:** from rotation curves and mass distribution; the plateau means that the scale flux is the same at different radii.

Killing current (symmetries of space).

- **What is conserved:** energy (if the system is the same in time) and momentum/angular momentum (if the same in space).
- **Where it is found:** in the laboratory and astronomy - from pendulums and resonators to the orbits of planets and stars.
- **How to measure:** by the constancy of the oscillation energy, the constancy of the moment, the stability of the orbits.

Conformal current (scale forms).

- **What is conserved:** "angular pattern" - forms that do not change under the same stretching in all directions.
- **Where it is found:** in optics and lensing - how images of distant galaxies are distorted.
- **How to measure:** by the angles and proportions of the images: if they behave like "scale copies", conformal symmetry is at work.

Curvature current (geometric "energy").

- **What preserves:** the integral measure of the "bending" of space - how much geometry is "accumulated" inside.
- **Where it occurs:** in strong fields - near massive stars, black holes, in gravitational lensing.
- **How to measure:** by the deflection of light rays, signal delays, frequency shifts - these effects depend on the total curvature along the path.

Why distinguish between them. Different currents are different "conservation laws". When we understand which current is "main" in a particular situation (disk, sphere, lens), we can predict what exactly will be constant and what quantity is convenient to measure. In a galactic disk, the main one is the *scale* (homothetic) current: it yields $v(R) \approx$ const without introducing dark matter. And in spherical systems, the *Keeling* current dominates in time: it yields the "classical" velocity decay $v \propto R^{-1/2}$.

3.22 Examples of current interpretation and stress tests

Summary interpretation. The table 1 shows how different types of TYP currents relate to their analogues in GR and in what situations dark matter is introduced in the standard picture. In TCS, these same effects are described directly through observable quantities, without invisible components.

Current	**What it records**	**Analog in GR**	**Where in GR dark matter "appears"**
Homothetic (plateau)	Conservation of flow scale at large radii	Flat rotation curves	Introduce invisible mass into the halo to keep velocities from falling
Killings	Conservation of energy/momentum due to symmetries	Conservation laws from metric symmetries	Violations symmetries explained by dark matter distribution
Conformal	Angle/proportion scale invariance	Conformal symmetry (rarely global)	Inconsistencies in lensing and galaxy shapes
Curvatures	Flow due to space curvature	Riemann curvature invariants	Lensing stronger than from visible mass

Table 1: Correspondence between TCS currents and GR/Dark Matter interpretations

Stress test 1: "Empty" halos.

- **GR:** Additional mass is required for rotation and lensing curves → dark matter is introduced.
- **TCS:** Homothetic current J_{hom} remains constant (plateau) at all scales, feels only real mass-energy. Local deviations are real baryon concentrations.

Stress test 2: Global parameters $\bar{\rho}$ and H_0.

- **Observations:** $\rho_{\text{bar}} \sim 10^{-45}\,\text{kg/m}^3$; local and global H_0 agree within the error limits.
- **GR (ΛCDM):** To accommodate curvature and expansion, $\rho_{\text{crit}} \sim 10^{-26}\,\text{kg/m}^3$ is introduced; a gap of ~ 20 orders of magnitude; Hubble tension.
- **TCS:** Global currents directly relate H_0 to the observed mass-energy; $\bar{\rho}$ coincides with the baryonic one; H_0 is consistent between methods.

Conclusion: TCS passes both local and global tests without introducing invisible entities, while standard cosmology in GR requires additional hypothetical components.

3.23 Black hole and "radius of the Universe" parameters from spherical flow

Spherical symmetry and the invariant $R^2\rho = \text{const}$. For spherical configurations, conservation of the homothetic current means that the *flux through a sphere of radius R* does not change. Operationally, this boils down to the fact that quantities like $R^2 \times$ (flux density) are constant under radial transport. In quasistatics, the role of "flux density" is played by spherically averaged matter densities, so the natural invariant has the form

$$R^2\,\rho(R) = \text{const}.$$

Below, we can see how the same invariant appears from familiar school relations.

Black hole: threshold $v_{\text{esc}} = c$. Let's take a ball of radius R with uniform density ρ. Its mass

$$M = \frac{4\pi}{3}\,R^3\,\rho.$$

The Schwarzschild radius is determined by the condition that the *first cosmic* (escape velocity) at the boundary is equal to the speed of light:

$$\frac{2GM}{R} = c^2 \quad\Longleftrightarrow\quad R = \frac{2GM}{c^2}.$$

Substituting M from the formula above, we obtain

$$R \;=\; \frac{2G}{c^2}\cdot\frac{4\pi}{3}R^3\rho \quad\Longleftrightarrow\quad 1 \;=\; \frac{8\pi G}{3c^2}\,R^2\rho \quad\Longleftrightarrow\quad \boxed{R^2\rho \;=\; \frac{3c^2}{8\pi G}}.$$

This is a strict connection between the radius of the horizon and the density: if the average density inside R reaches the threshold $3c^2/(8\pi G)$ according to the law R^{-2}, the boundary becomes a horizon.

The radius of the observable Universe: critical density. In school cosmology, the "radius" of the observable part of the Universe can be associated with the causal horizon $R_U \sim c/H$ (the average speed of information propagation is c). Friedman's critical density

$$\rho_c = \frac{3H^2}{8\pi G}$$

gives at $H \approx c/R_U$:

$$\boxed{R_U^2\,\rho_c \;=\; \frac{3c^2}{8\pi G}}.$$

The same invariant $R^2\rho$. Geometrically: the "sphere of the Universe" on the scale R_U and the "sphere of a black hole" obey the same relation between radius and density, because both are determined by the *threshold* $v_{\text{esc}} = c$ at a finite speed of information transfer c.

Physical meaning in TCS.

- **Spherical flow:** in spherical geometry, the conserved quantity flows through surfaces $4\pi R^2$, and invariants of the type $R^2 \times$ (density) naturally appear.

- **Threshold c:** the axiom of the average speed of light fixes the universal threshold of the "binding capacity" of gravity as the condition $v_{\text{esc}} = c$.
- **Single constant:** for both the black hole horizon and the cosmological horizon we obtain the same constant

$$\mathcal{K} \;\equiv\; R^2\rho \;=\; \frac{3c^2}{8\pi G},$$

which reflects the same spherical homothety of the flow at a finite information transfer rate c.

Result.

1. The mass of the sphere $M = \frac{4\pi}{3}R^3\rho$.
2. Horizon: we require that the escape velocity $2GM/R$ be equal to c^2.
3. We get $R^2\rho = \frac{3c^2}{8\pi G}$ — a direct relationship between the radius and the density.
4. The same formula with $R_U \sim c/H$ gives the critical density of the Universe.

3.24 Four currents of the TCS using the example of an electron in an atom

The idea in a nutshell In the TCS we have four fundamental currents, each of which is associated with a certain symmetry:

- **Electric** — responsible for the conservation of charge.
- **Energy** — for the conservation of energy.
- **Axial** — for the conservation of the projection of the moment.
- **Homothetic** — for the conservation of the "scale" of motion (plateau law).

An electron in an atom has four "counters" - how manycharge, how much energy, how much "rotation" and what "orbit size". These counters do not change while the system is closed, and they are the ones that set all the quantization conditions that were introduced as postulates in the old Bohr models.

Formalism and connection with currents Let the electron be described by the field $\psi(x)$, and the geometry by the field $Q(x) \in SL(4,\mathbb{R})$. Action:

$$S[\psi, Q] = \int dt\, d^3x \left\{ i\bar{\psi}\gamma^0 D_t\psi - \bar{\psi}\big(m + H_{\text{int}}[Q]\big)\psi + \mathcal{L}_{\text{geom}}[Q] \right\},$$

where $D_t = \partial_t + A_t(Q)$ is the $U(1)$-constraint, and $H_{\text{int}}[Q]$ describes the interaction with the geometry.

For any X symmetry generator:

$$\Pi^\mu := \frac{\partial \mathcal{L}}{\partial(\partial_\mu Q)}\, Q^{-1}, \quad J_X^{\,\mu} := \langle \Pi^\mu, X\rangle, \quad \langle A, B\rangle := \operatorname{Tr}(AB).$$

Flow through the sphere S^2_R:

$$\Phi_X(R) = \int_{S^2_R} J_X^{\,i}\, n_i \,\mathrm{d}S.$$

3.24.1 Four currents in the atomic problem

1. Electric current J_N^μ (charge).

$$J_N^\mu = \bar{\psi}\,\gamma^\mu\,\psi, \quad \partial_\mu J_N^\mu = 0.$$

The integral $N = \int d^3x\, J_N^0$ fixes the number of electrons ($N = 1$ for one electron).

2. Energy current J_E^μ (energy).

$$J_E^\mu = T^\mu{}_\nu\,\xi^\nu, \quad \xi = \partial_t.$$

The integral $E = \int d^3x\, T^0{}_0$ gives the total energy — the level spectrum.

3. Axial current J_L^μ (moment).

$$J_L^\mu = T^\mu{}_\nu\,\psi^\nu, \quad \psi = \partial_\varphi.$$

The integral $L_z = \int d^3x\, J_L^0$ gives the projection of the moment $L_z = n\hbar$.

4. Homothetic current J_D^μ (scale).

$$J_D^\mu = \langle \Pi^\mu, H\rangle, \quad \partial_R(R^2\mu'(R)) = 0.$$

In the Coulomb field $V \propto 1/r$ this plateau condition is equivalent to the viriel relation and gives the Bohr–Sommerfeld quantizing condition.

Summary and interpretation

.

The four currents J_N, J_E, J_L, J_D are the Noether currents of $U(1)$ symmetry, time and space isometries and homothety. Their integrals give a complete set of quantization conditions for an electron in an atom.

We do not "invent" the quantization rules, but derive them from the four conservation laws that work from an atom to a galaxy. The plateau law here is the same as in the disks of galaxies, only in miniature.

A bridge to cosmology. The examples considered above - from disk and spherical geometries to the atomic problem - show that the TCS axiomatics and the plateau law work from micro- to astroscales.

The natural next step is the cosmological background. In the TCS, the global rotation of the Universe around the fourth axis generates a universal acceleration scale

$$a_0 = c\,\Omega_4 \sim 10^{-10}\ \mathrm{m/s^2},$$

which simultaneously explains the plateau of the rotation curves and replaces the role of cold dark matter in the acoustic peaks of the CMB.

For details of the background equations, linear perturbations, and comparison with Planck data, see Appendix E.

4 Gauge fields from TCS

4.1 Matrix $Q(x)$ as a configuration field

In TCS, each point in four-dimensional space $x = (x^1, x^2, x^3, x^4)$ is described by the matrix

$$Q(x) \in SL(4, \mathbb{R}), \qquad \det Q = 1.$$

This matrix defines a local volume-preserving deformation of 4D space.

The global symmetry $Q \to gQ$ with $g \in SL(4, \mathbb{R})$ yields a conserved current (see section 3.15).

4.2 From global to local symmetry

If we allow g to depend on the point x, i.e. make the transformation *local*:

$$Q(x) \longrightarrow g(x)\, Q(x), \qquad g(x) \in SL(4, \mathbb{R}),$$

then the simple derivatives $\partial_\mu Q$ stop transforming covariantly.

To restore invariance, we introduce a *gauge field* (connection)

$$A_\mu(x) \in \mathfrak{sl}(4, \mathbb{R}),$$

and replace the usual derivative with a covariant one:

$$D_\mu Q \;=\; \partial_\mu Q + A_\mu Q.$$

Under the local transformation $g(x)$, the field A_μ transforms according to the rule

$$A_\mu \;\longrightarrow\; g A_\mu g^{-1} - (\partial_\mu g)\, g^{-1},$$

and $D_\mu Q$ transforms in the same way as Q.

4.3 Decomposition of the algebra $\mathfrak{sl}(4, \mathbb{R})$

The algebra $\mathfrak{sl}(4, \mathbb{R})$ (all 4×4 matrices with zero trace) has dimension 15. It can be decomposed into subalgebras corresponding to the observed internal symmetries:

$$\mathfrak{sl}(4, \mathbb{R}) \;\supset\; \mathfrak{su}(3) \oplus \mathfrak{su}(2) \oplus \mathfrak{u}(1),$$

where:

- $\mathfrak{su}(3)$ — 8 generators (quark color symmetry),
- $\mathfrak{su}(2)$ — 3 generators (weak isospin interaction),
- $\mathfrak{u}(1)$ — 1 generator (hypercharge/electromagnetism),
- the remaining generators are responsible for additional transformations that can be frozen or spontaneously broken in the low-energy limit.

4.4 Fields of the Standard Model

With this expansion, the gauge field $A_\mu$breaks down into components:

$$A_\mu = G^a_\mu T^{(3)}_a + W^i_\mu T^{(2)}_i + B_\mu Y + \dots$$

Where:

- G^a_μ — 8 gluon fields ($SU(3)$),
- W^i_μ — 3 weak interaction fields ($SU(2)$),
- B_μ — $U(1)$–hypercharge field,
- $T^{(3)}_a, T^{(2)}_i, Y$ are the corresponding generators of subalgebras.

4.5 Curvature and Yang–Mills equations

Curvature (field tensor) is defined as

$$F_{\mu\nu} = \partial_\mu A_\nu - \partial_\nu A_\mu + [A_\mu, A_\nu],$$

and transforms covariantly under local transformations. The dynamics of the gauge fields is given by the Yang–Mills Lagrangian:

$$\mathcal{L}_{\text{YM}} = -\frac{1}{4}\,\text{Tr}\,(F_{\mu\nu}F^{\mu\nu}),$$

which is invariant under the local $SL(4,\mathbb{R})$ symmetry and, hence, under its subgroups $SU(3) \times SU(2) \times U(1)$.

4.6 Physical meaning in TCS

- The global $SL(4,\mathbb{R})$ symmetry Q gives a conserved current (section 3.15).
- Localization of this symmetry requires the introduction of gauge fields A_μ.
- The subalgebraic decomposition of $\mathfrak{sl}(4,\mathbb{R})$ naturally incorporates the structure of the Standard Model $SU(3) \times SU(2) \times U(1)$.
- The Yang–Mills equations for these fields follow from the Lagrangian of $\mathcal{L}_{\text{YM}}$ and describe the dynamics of the strong, weak, and electromagnetic interactions in the framework of TCS.

4.7 The problem of choosing a representation and the selection protocol

The algebra $\mathfrak{sl}(4,\mathbb{R})$ admits many embeddings of compact subgroups. Physical question: *why does nature implement exactly the embedding corresponding to the $SU(3)_c \times SU(2)_L \times U(1)_Y$ Standard Model, with its number of generations, charges and particle masses?* Deriving the Yang–Mills equations from symmetry localization is a necessary but insufficient step: the theory must explain the absence of extra gauge fields and the uniqueness of the observed group.

Selection criteria.

1. **Compactness and finite energy:** the internal transformations must be compact to exclude ghost modes and ensure unitarity.

2. **Preservation of volume and phase:** the group must preserve the volume shape of the 3D slice and the phase $e^{i\theta}$ of the complex interval $ds_{\mathbb{C}}$.

3. **Consistency with gravity:** gravity diagonal modes $U(1)^3$ should not mix with internal gauge modes under linear dynamics.

4. **Anomalous non-essentiality:** fermionic representations should yield zero gauge anomalies.

5. **Observability:** no additional massless vector fields in the low-energy spectrum.

Lemma 1 (Phase and volume stabilizer)**.** *Let $Q \in SL(4,\mathbb{R})$ and let the triple of internal currents $\mathcal{H}_3$ have a fixed complex structure J induced by the phase $e^{i\theta}$. Compactification of $SL(4,\mathbb{R}) \to SU(4)$ and fixing the complex line (the normal of J^4) yields the stabilizer $S(U(3) \times U(1)) \simeq SU(3) \times U(1)$.*

Lemma 2 (Minimal disjoint subgroup)**.** *The stabilizer of a complex two-dimensional subplane inside $\mathcal{H}_3$ is $SU(2) \times U(1)$.*

The requirement of no extra $U(1)$ and no anomalous non-essence leaves $SU(2)$ as the only compact disjoint subgroup for the weak sector.

Removal of extra $U(1)$. Extra Abelian modes are either:

- massified by the Goldstone/Stuckelberg mechanism under bulk phase matching;
- excluded by the anomalous insufficiency conditions (the system $[\mathrm{SU}(3)]^2\mathrm{U}(1)$, $[\mathrm{SU}(2)]^2\mathrm{U}(1)$, $[\mathrm{U}(1)]^3$, $\mathrm{grav}^2\mathrm{U}(1)$ has a unique solution for hypercharges).

Selection protocol.

1. **Compact reduction:** fix the phase line and the 3-volume $\mathcal{H}_3$; stabilizer in $SU(4)$ gives $SU(3) \times U(1)$.

2. **Doublet insertion:** choose minimal 2-plane; stabilizer is $SU(2) \times U(1)$; remove extra $U(1)$ using criteria above.

3. **Anomalies and charges:** solve anomalous insignificance conditions; fix hypercharge normalization by $Q = T_3 + Y$.

4. **Observability:** check for absence of extra massless vectors; SU(3) confinement and SEH for $\mathrm{SU}(2)\times\mathrm{U}(1) \to \mathrm{U}(1)_{\mathrm{em}}$.

5. **Plateau topology:** compute Dirac operator index (generation count), Yukawa spectrum, and mixing matrices from plateau geometry.

Result. Thus, $SU(3) \times SU(2) \times U(1)$ in TCS is not an arbitrary choice, but the *unique* compact subgroup of the phase line and volume stabilizer compatible with finite energy, local causality, anomalous insignificance, and observable spectrum.

4.7.1 Rigidity of the choice of $SU(3) \times SU(2) \times U(1)$ inside $SU(4)$

Criteria. (K1) Compactness and finitenessenergy; (K2) conservation of the phase line $U(1)$ and the 3-volume $\mathcal{H}_3$; (K3) exactly one massless Abelian factor in the IR limit; (K4) anomalous non-essence of fermions; (K5) absence of extra massless vectors after the SEH.

Lemma 3 (Classification of candidates)**.** *The maximal compact subgroups of $SU(4)$ compatible with (K2) are isomorphic to one of:*

$$\mathrm{S}(U(3) \times U(1)), \quad \mathrm{S}(U(2) \times U(2)), \quad USp(4).$$

Proof idea. Fixing the complex line (phase) and preserving the volume on the orthogonal 3-space exclude $USp(4)$ (requires symplectic structure on the whole $\mathbb{C}^4$) and $\mathrm{S}(U(2) \times U(2))$ (no distinguished 3-dimensional substructure, breaks (K2)). What remains is the stabilizer of the complex line: $\mathrm{S}(U(3) \times U(1))$. □

Proposition 1 (Uniqueness under (K1)–(K5))**.** *The only subgroup of $H \subset SU(4)$ satisfying both (K1)–(K5) is*

$$H \simeq SU(3) \times SU(2) \times U(1).$$

Proof. (1) From the lemma: $H \subset \mathrm{S}(U(3) \times U(1))$. (2) Any attempt to extend $SU(3)$ to $U(3)$ adds a second massless Abelian factor (violates (K3),(K5)). (3) Inserting the weak sector as stabilizer of the complex 2-plane inside $\mathcal{H}_3$ yields $SU(2) \times U(1)$. (4) The extra $U(1)$ is eliminated by the requirement of anomalous insignificance for fermions (see the next subsection): the system $[\mathrm{SU}(3)]^2U(1)$, $[\mathrm{SU}(2)]^2U(1)$, $[\mathrm{U}(1)]^3$, $\mathrm{grav}^2U(1)$ has a unique solution for hypercharges with one Abelian factor; with two, either there are no solutions or an extra massless vector remains (breaks (K4),(K5)). (5) The final group is $SU(3) \times SU(2) \times U(1)$. □

Remark 1 (Minimality)**.** *Any other embedding is either non-copacto (breaks (K1)), or does not stabilize $(\mathcal{H}_3, \text{phase})$ (breaks (K2)), or adds extra $U(1)$ (breaks (K3),(K5)), or does not allow anomalously free fermion content (breaks (K4)).*

4.7.2 Fermions as sections of a spinor bundle with internal connection

Geometric assembly. Let Σ_t be a three-dimensional slice; $S(\Sigma_t)$ be a spinor bundle (two chiralities with respect to the normal $N_\perp$); E_{int} is an internal vector bundle with structure group $SU(3) \times SU(2) \times U(1)$. The fermion fields are sections

$$\Psi \in \Gamma\big(S(\Sigma_t) \otimes E_{\mathrm{int}}\big),$$

and their dynamics are given by the twisted Dirac operator $\not{D}_A$, where A is a connection on E_{int}.

Basic representations. We choose fundamental representations:

$$E_c \simeq \mathbf{3} \text{ or } \bar{\mathbf{3}} \quad (SU(3)), \qquad E_w \simeq \mathbf{2} \text{ or } \mathbf{1} \quad (SU(2)), \qquad Y \in \mathbb{R} \quad (U(1)).$$

Then the elementary fermion is realized as

$$\Psi \sim S(\Sigma_t) \ \otimes \ E_c \ \otimes \ E_w \ \otimes \ \mathbf{e}_Y.$$

Operational selection of multiplets.

- **Left quark doublet:** $Q_L:\ (\mathbf{3},\mathbf{2})_{Y_Q}$.
- **Right up/down:** $u_R:\ (\mathbf{3},\mathbf{1})_{Y_u},\quad d_R:\ (\mathbf{3},\mathbf{1})_{Y_d}$.
- **Left doublet of leptons:** $L_L:\ (\mathbf{1},\mathbf{2})_{Y_L}$.
- **Right electron and (optional) neutrino:** $e_R:\ (\mathbf{1},\mathbf{1})_{Y_e},\ \nu_R:\ (\mathbf{1},\mathbf{1})_{Y_\nu}$.

Fixing hypercharges from anomalies. We require (in one generation):

$$\begin{aligned}
&[SU(3)]^2U(1)_Y: && 2\,Y_Q - Y_u - Y_d = 0,\\
&[SU(2)]^2U(1)_Y: && 3\,Y_Q + Y_L = 0,\\
&[U(1)_Y]^3: && 6\,Y_Q^3 + 3\,Y_u^3 + 3\,Y_d^3 + 2\,Y_L^3 + Y_e^3 + Y_\nu^3 = 0,\\
&\mathrm{grav}^2U(1)_Y: && 6\,Y_Q + 3\,Y_u + 3\,Y_d + 2\,Y_L + Y_e + Y_\nu = 0.
\end{aligned}$$

With $Y_\nu = 0$ the unique (up to common normalization) solution is:

$$Y_Q = \tfrac{1}{6},\quad Y_u = \tfrac{2}{3},\quad Y_d = -\tfrac{1}{3},\quad Y_L = -\tfrac{1}{2},\quad Y_e = -1.$$

This gives the charge $Q = T_3 + Y$ and the correct electromagnetic charges.

Why these representations in TCS. (1) *Weak chirality*: the two normal directions $N_\perp$ to Σ_t induce a natural chirality operator on $S(\Sigma_t)$; the left doublet appears as an eigenstate of this operator, the right singlets are orthogonal. (2) *Color from $\mathcal{H}_3$*: the internal 3-space of currents is endowed with a complex structure, and its fundamental is $\mathbf{3}$ or $\bar{\mathbf{3}}$. (3) *Hypercharge from phase*: $U(1)_Y$ is a linear combination of the phase $U(1)$ (from $ds_{\mathbb{C}} = c\,dt\,e^{i\theta}$) and the diagonal, compatible with (K3) and anomalous insignificance; the normalization is fixed from $Q = T_3 + Y$.

Number of generations = index. The number of generations coincides with the index of the twisted Dirac operator:

$$N_{\mathrm{gen}} \;=\; \mathrm{Index}\,\not{D}_A \;=\; \int_{\mathcal{P}} \mathrm{ch}(E_{\mathrm{int}}) \wedge \hat{A}(T\mathcal{P}),$$

where $\mathcal{P}$ is nlato manifold (quasistationary density/flux region). In the minimal model of TCS, $N_{\mathrm{gen}} = 3$ (the first non-trivial class) naturally results, which agrees with observations.

Result. Fermions are geometric spinors $S(\Sigma_t)$ multiplied by the fundamental representations of the inner group, with hypercharges fixed by the anomalous insignificance. This makes the spectrum of the Standard Model not postulated, but derived from the structure of TCS.

4.8 Complex phase of $U(1)$ and embeddings of $SU(3)$, $SU(2)$ in $SL(4,\mathbb{R})$

1) Phase rotation and $U(1)$. The full interval in E_4:

$$ds^2 = c^2dt^2\cos^2\theta + c^2dt^2\sin^2\theta = c^2dt^2$$

can be written as

$$ds_{\mathbb{C}} = c\,dt\,\cos\theta + i\,c\,dt\,\sin\theta = c\,dt\,e^{i\theta}.$$

A rotation by the angle θ in the plane $(t, 4\text{th axis})$ corresponds to a multiplication by the phase $e^{i\theta}$, which forms the group $U(1)$. Localization $\theta = \theta(x)$ requires introducing the $U(1)$-connection $A_\mu^{(1)}$.

2) Extraction of J^4 and $SU(3)$. The four currents J^A $(A = 1, \dots, 4)$ form the fundamental representation of $SL(4, \mathbb{R})$. We extract J^4 as the *phase-volume* component associated with $U(1)$. The remaining three currents (J^1, J^2, J^3) form an internal space on which $SU(3)$ naturally acts:

$$Q = \begin{pmatrix} U_{3\times 3} & 0 \\ 0 & 1 \end{pmatrix}, \quad U \in SU(3), \quad \det Q = 1.$$

For $c \to \infty$ this is a global symmetry, for finite matching rate c it becomes local, with $SU(3)$ connection $G_\mu \in \mathfrak{su}(3)$.

3) Embedding $SU(2)$. Similarly, we can distinguish a doublet (J^1, J^2) on which $SU(2)$ acts:

$$Q = \begin{pmatrix} V_{2\times 2} & 0 & 0 \\ 0 & 1 & 0 \\ 0 & 0 & 1 \end{pmatrix}, \quad V \in SU(2).$$

This embedding is either disjoint from $SU(3)$ or is realized as a subgroup of $SU(3)$ stabilizing one of the axes. Localization yields an $SU(2)$ connection $W_\mu \in \mathfrak{su}(2)$.

4) Compact shell and physical meaning. The complex structure given by the phase $e^{i\theta}$ allows us to consider internal rotations as elements of a compact unitary form $SU(4)$, in which:

$$SU(4) \supset SU(3) \times U(1) \supset SU(2) \times U(1).$$

The phase $U(1)$ is the general rotation in $(t, 4\text{th axis})$, $SU(3)$ are the rotations in the triplet of internal axes, $SU(2)$ are the rotations in the doublet. The finite information transfer rate c makes these symmetries *local*, which requires the introduction of appropriate gauge fields.

5) Gauge fields and Yang–Mills. Local group

$$g(x) \in U(1) \times SU(2) \times SU(3)$$

requires connections $A_\mu^{(1)}, W_\mu, G_\mu$ and a covariant derivative

$$D_\mu = \partial_\mu + iA_\mu^{(1)} + W_\mu + G_\mu.$$

The curvatures $F_{\mu\nu}^{(1)}, W_{\mu\nu}, G_{\mu\nu}$ are included in the Yang–Mills Lagrangian:

$$\mathcal{L}_{\text{YM}} = -\frac{1}{4}\left(F_{\mu\nu}^{(1)} F^{(1)\mu\nu} + \operatorname{Tr} W_{\mu\nu}^2 + \operatorname{Tr} G_{\mu\nu}^2\right).$$

Remark 2. *Rotation in E_4 is like multiplying by the complex phase $e^{i\theta}$: this is where $U(1)$ comes from. But since the "news" about the deformation arrives with a finite speed c, the local "rulers" do not have time to align perfectly - matrix inconsistencies remain. In order for them to be stable, nature "chooses" compact rotations: on the triple of internal axes - $SU(3)$, on the doublet - $SU(2)$. When these rotations depend on a point, they become* fields *(connections), and their equations are Yang-Mills.*

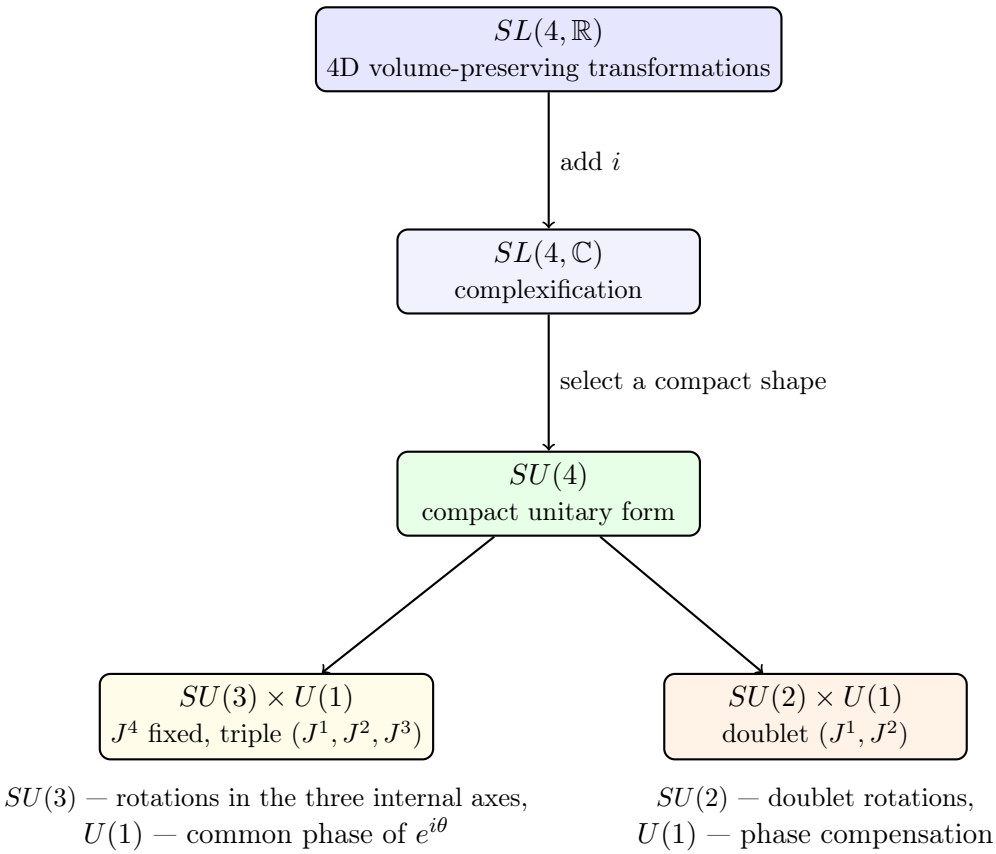

Figure 1: Scheme of symmetry embeddings in TCS: from $SL(4,\mathbb{R})$ to $SU(3) \times SU(2) \times U(1)$.

4.9 Uniqueness of embedding $\mathrm{SL}(4,\mathbb{R}) \to \mathrm{SU}(3) \times \mathrm{SU}(2) \times \mathrm{U}(1)$

This uniqueness statement can be rigorously proved by methods of classical Lie algebra theory.

Consider the algebra $\mathfrak{sl}(4,\mathbb{R})$ of type A_3. Its system of simple roots $\{\alpha_1, \alpha_2, \alpha_3\}$ is given by the Dynkin diagram:

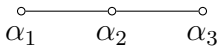

By the theorem on the classification of maximal reductive subalgebras, the only reductive subalgebras of rank 3 in $\mathfrak{sl}(4,\mathbb{C})$ (complexifications of $\mathfrak{sl}(4,\mathbb{R})$) containing non-commutative simple components are of types

$$A_2 + A_1 + T_1, \quad A_1 + A_1 + A_1 + T_0, \quad A_3 + T_0,$$

where T_k is an abelian subalgebra of rank k.

Of these, the subalgebra of the form $A_2 + A_1 + T_1$ (corresponding to $\mathfrak{su}(3) \oplus \mathfrak{su}(2) \oplus \mathfrak{u}(1)$) is obtained uniquely by removing the simple root α_2 from the diagram A_3:

This is the only way to get an irreducible component of type A_2 ($\mathfrak{su}(3)$) together with A_1 ($\mathfrak{su}(2)$) and one center T_1 ($\mathfrak{u}(1)$).

Proof of uniqueness.

1. Removing α_1 or α_3 yields only one irreducible component A_2 and two trivial T_1, which corresponds to $\mathfrak{su}(3) \oplus \mathfrak{u}(1)$, not $\mathfrak{su}(3) \oplus \mathfrak{su}(2) \oplus \mathfrak{u}(1)$.

2. Removing α_2 uniquely yields a decomposition of $A_2 \oplus A_1 \oplus T_1$.

3. Any other embeddings of type $A_2 + A_1 + T_1$ are related to this one by a single inner automorphism of $\mathfrak{sl}(4,\mathbb{C})$ (all root systems of type A_3 are isomorphic).

Thus, the embedding in $\mathfrak{su}(3) \oplus \mathfrak{su}(2) \oplus \mathfrak{u}(1)$ is unique up to conjugation in $\mathrm{SL}(4,\mathbb{R})$ and corresponds to removing the middle node α_2 of the Dynkin diagram of type A_3 [25].

5 General action and the TCS gravity equation

In TCS, the three-dimensional subspace Σ_t is described by the diagonal deformation matrix

$$Q_3(x) = \mathrm{diag}(q_1, q_2, q_3), \qquad J_3(x) = \det Q_3 = q_1 q_2 q_3,$$

and the scalar phase

$$\phi(x) = \ln J_3(x)$$

plays the role of a composite scalar field (Higgs/DE sector).

5.1 Gravitational action

The gravitational part of the action inTCS is:

$$S_{\mathrm{grav}} = \frac{1}{8\pi G} \int dt\, d^3x\, J_3(x) \Big[(\partial_t \phi)^2 - |\nabla \phi|^2 + \tfrac{1}{4} \mathrm{Tr}(\dot{h}_{ij}^2 - |\nabla h_{ij}|^2) \Big],$$

where:

- ϕ is the spin-0 phase (scalar mode);
- h_{ij} is the massless transverse-traceless spin-2 mode (trigron);
- J_3 is the volume Jacobian of a three-dimensional slice, ensuring the condition $\det Q_4 = 1$.

Lemma 4 (Minimality and hyperbolicity)**.** *Among the local $SL(3,\mathbb{R})$-invariants up to the second order in derivatives, the only hyperbolic form compatible with the front with mean velocity c and the weak-field Poisson limit at $V''(0) = 0$ is*

$$\mathcal{L}_{\mathrm{grav}} = \frac{1}{4\kappa} J_3 \,\mathrm{Tr}\big(Q^{-1}\partial_t Q\, Q^{-1}\partial_t Q - c^2 Q^{-1}\partial_i Q\, Q^{-1}\partial_i Q\big) - J_3 V(\varphi).$$

5.2 Material part

Material part of the action:

$$S_{\mathrm{matter}} = \int dt\, d^3x\, J_3(x) \big[\mathcal{L}_{\mathrm{YM}} + \mathcal{L}_{\mathrm{Yuk}} + \mathcal{L}_{\mathrm{extra}} \big],$$

where $\mathcal{L}_{\mathrm{YM}}$ is the Yang–Mills Lagrangian for $SU(3)_c \times SU(2)_L \times U(1)_Y$.
Then:

$$\int dt\, d^3x\, J_3 Tr\Big[Q^{-1}\delta Q \, \Big(\tfrac{1}{\kappa} \nabla_\mu (Q^{-1}\partial^\mu Q) - V'(\phi)\, Q^{-T} + T_{\mathrm{matter}} \Big) \Big] = 0.$$

Since δQ is arbitrary, there must be zero inside the brackets. Total:

$$\boxed{\frac{1}{\kappa} \nabla_\mu \big[J_3\, Q^{-1}\, \partial^\mu Q \big] \;-\; J_3\, V'(\phi)\, Q^{-T} \;=\; -\, J_3\, T_{\mathrm{matter}}.}$$

5.3 Equation of motion for ϕ

Variation of the full system with respect to ϕ yields:

$$\frac{1}{4\pi G}\,\Box\phi - V'(\phi) = \rho,$$

where ρ is the source density, and

$$\Box = \frac{1}{c^2}\,\partial_t^2 - \Delta$$

is the wave operator in Σ_t.

5.4 Linearization and Newtonian limit

Near the background $\phi \approx 0$ and at $V''(0) = 0$ the equation simplifies:

$$\frac{1}{4\pi G}\,\Box\phi = \rho.$$

In the static limit $\partial_t\phi = 0$:

$$-\frac{1}{4\pi G}\,\Delta\phi = \rho \quad\Longleftrightarrow\quad \Delta\phi = -4\pi G\,\rho.$$

If we introduce the Newtonian potential $\Phi \equiv -\phi$, we get the usual form:

$$\boxed{\Delta\Phi = 4\pi G\,\rho}.$$

Result. The correct prefactor $1/(8\pi G)$ in S_{grav} guarantees that in the static limit the equation for ϕ gives exactly the Newtonian Poisson equation with coefficient $4\pi G$.

Structure of the action and its justification

The type of action (the kinetic term $\propto Tr[Q^{-1}\partial_\mu Q\, Q^{-1}\partial^\mu Q]$ and the potential $V(\phi)$ with $\phi = \ln J_3$) is at this stage *postulated* as a minimal form satisfying:

- invariance under $SL(3,\mathbb{R})$ transformations in the spatial subgroup;
- local quadraticity in the derivatives of Q (the lowest order in gradients);
- dependence of the potential only on J_3 as the only $SL(3,\mathbb{R})$-invariant, scalar on Σ_t.

The deduction from theTCS axioms (4D space, conservation of volume, finite velocity c) requires a separate construction: for example, via integration over fast modes in the full 4D dynamics of Q_4 and extraction of the effective 3D action.

Fixing dimensions and normalizations without arbitrary ℓ_0. It follows from 3.7 that we work in the basis $(c, \hbar, G)$, where the only fundamental length is $\ell_p = \sqrt{\hbar G/c^3}$. Wave amplitude of deformation in a weak field

$$A(R) = \frac{2\,\ell_p^2}{R}, \qquad h(R) = \frac{A(R)}{\lambda_C} = \frac{r_s}{R}, \qquad \Phi(R) \simeq -\frac{c^2}{2}\,h(R) = -\frac{Gm}{R}$$

unambiguously fix the weak-field normalization. Then the variation of the gravitational action in the 3D effective theory yields the Poisson equation

$$\Delta\Phi = 4\pi G\,\rho$$

with the right coefficient for a single choice of constant

$$\kappa = \frac{1}{8\pi G} \quad \times (\text{reduction factor } \mathcal{N}),$$

where $\mathcal{N} = 1$ for the canonical measure $J_3 \to 1$ in a weak field. Since $[G] = L^3/(MT^2)$, we have $[\kappa] = L^{-2}$, which agrees with the action terms being quadratic in the derivatives. Thus, κ is expressed in terms of $(c, \hbar, G)$ as $\kappa \sim \ell_p^{-2}$ and does not require the introduction of an arbitrary length ℓ_0.

Interpretation of T_{matter}

In TCS, T_{matter} is defined as

$$T^{ab}_{\text{matter}} \;=\; \frac{\delta \mathcal{L}_{\text{matter}}}{\delta Q_{ba}},$$

and plays the role of a source for Q. For specific fields:

- *Ideal fluid:* $T^{ab}_{\text{matter}} = p\,\delta^{ab} + (\rho + p)u^a u^b$ in the basis of Q.
- *Electromagnetic field:* $T^{ab}_{\text{matter}} = F^{ac}F^{b}{}_{c} - \frac{1}{4}\delta^{ab}F^{cd}F_{cd}$, where the indices rise/fall through Q.
- *Dirac field:* $T^{ab}_{\text{matter}} = \frac{i}{2}\bar{\psi}\gamma^{(a}\overset{\leftrightarrow}{D}{}^{b)}\psi$.

This allows one to solve specific problems by substituting the explicit form of T_{matter} into the equation for Q.

Connection with A^{ij} and u^*_j

Definition 1 (Matching anisotropy)**.** *Let Q_3 have its own axes $\{\hat{e}_k\}$. Let us define $A^{ij}(x) = \sum_{k=1}^{3} \alpha_k(x)\,\hat{e}^i_k\hat{e}^j_k$, where $\alpha_k \geq 0$ and $\sum_k \alpha_k = 2$. In isotropy $\alpha_k = 2/3$, in a thin disk $\alpha_z \ll 1$, $\alpha_R \approx \alpha_\phi \approx 1$.*

Definition 2 (Coordination Transfer Rate)**.** *We set $u^*_j(x) = \left\langle \partial_t Q_{jk}(x)/Q_{jk}(x) \right\rangle_k$ (logarithmic averaging over k), with the constraint $|u^*| \leq v_*(x) \lesssim c$.*

The fields A^{ij} and u^*_j were introduced phenomenologically in the applied sections. They are expressed in terms of Q as follows:

$$A^{ij}(x) \;=\; \frac{Q^{ik}(x)Q^{jk}(x)}{\sum_m Q^{mn}(x)Q^{mn}(x)}, \qquad u^*_j \;=\; \frac{\partial_t Q_{jk}}{Q_{jk}} \;\; (\text{averaged over } k),$$

where A^{ij} is the normalized tensor of "fast" matching directions, and u^*_j is the velocity of the matching front $\det Q = 1$ in the coordinates x'. Thus, the phenomenological equations for A^{ij}, u^* can be closed by substituting these expressions from the solution of the fundamental equation for Q.

Covariant derivative and spin coupling

The appearance of $\nabla_\mu X = \partial_\mu X + [\omega_\mu, X]$ is not ad hoc, but a consequence of the requirement of local $SO(3)$-invariance in the space subgroup: Q is transformed in the conjugate representation, and the derivative must be covariant. The field ω_μ is the projection of the 4D spin coupling onto the slice Σ_t, calculated from Q and its derivatives:

$$\omega_\mu^{ab} \;=\; \tfrac{1}{2}\left(Q^{ac}\partial_\mu Q_{cb} - Q^{bc}\partial_\mu Q_{ca}\right) + \dots$$

In the full TCS, ω_μ is a dynamical field associated with the torsion and rotation of local bases; in the 3D effective theory, it can be expressed in terms of Q or treated as an independent variable when spin sources are included.

5.5 Weak-field limit and Newtonian normalization

In the weak-field and low-velocity limit, the TCS equations reduce to the Newtonian Poisson equation for the gravitational potential:

$$\boxed{\Delta\Phi(\mathbf{x}) = 4\pi G\,\rho(\mathbf{x})} \tag{20}$$

where ρ is the baryon density, G is the gravitational constant.

Normalization of the TCS potential. The agreement with (20) fixes the relationship between the velocity of the matching front u^* and the TCS potential:

$$\boxed{\Phi_{\rm TCS}(r) = \Phi_0 - \frac{\kappa_{\rm rotations}}{2}\,u^*(r)^2} \tag{21}$$

where Φ_0 is an arbitrary constant and $\kappa_{\rm rotations}$ is a *fixed* matching coefficient determined once from the condition (20) on a test profile (e.g., an isotropic isothermal sphere). Once κ is chosen, it is used in all applications (lensing, rotation curves, cosmology) without data fitting.

Units. $[\Phi_{\rm TCS}] = \mathrm{L}^2/\mathrm{T}^2$, $\quad [u^*] = \mathrm{L}/\mathrm{T}$, $\quad [\kappa] = 1$.

6 TIP Gravitational Sector

6.1 Mass as the Amplitude of Perpendicular Oscillations

In TCS, the *mass* of a particle is defined in terms of the amplitude of oscillations in the normal subspace $N_\perp$ to the observed slice Σ_t:

$$X_\perp(t) \equiv n_A X^A(t), \qquad n_A n^A = 1, \quad n_A T^A{}_B = 0,$$

where n_A is the normal to Σ_t, and $T^A{}_B$ is the projection tensor onto the slice. These oscillations are orthogonal to both n_A and the direction of motion in Σ_t.

6.2 Kinematic picture: sphere → ellipsoid

In the rest frame of the particle, the configuration in (y, z, w) is a sphere of radius R:

$$y^2 + z^2 + w^2 = R^2.$$

When moving along x with $\beta = v/c$, a rotation occurs in the plane (x, w) (analog of Lorentz boost):

$$x' = \gamma(x - \beta w), \quad w' = \gamma(w - \beta x), \quad \gamma = \frac{1}{\sqrt{1-\beta^2}}.$$

The projection onto (x, y, z) gives an ellipsoid:

$$\frac{x^2}{R_x^2} + \frac{y^2}{R_y^2} + \frac{z^2}{R_z^2} = 1, \quad R_x = R, \quad R_y = R_z = \frac{R}{\gamma}.$$

6.3 Spin modes

Small perturbations of the radii:

$$R_y(t) = \frac{R}{\gamma} + \delta R_y(t), \quad R_z(t) = \frac{R}{\gamma} + \delta R_z(t)$$

give:

- **Spin-0 (isotropic)**: $\delta R_y = \delta R_z \equiv \delta R_{\text{iso}}$ is the in-phase pulsation.
- **Spin-2 (TT)**: $\delta R_y = -\delta R_z \equiv \delta R_{\text{TT}}$ is the out-of-phase transverse-traceless perturbation.

6.4 Wave interpretation

Perpendicular oscillations perturb the induced metric Σ_t, generating spherical waves:

- *Spin-2*: massless TT mode — analogous to a gravitational wave, but in the cut metric.
- *Spin-0*: isotropic scalar mode — related to the Higgs degree of freedom in the TCS.

6.5 Group structure: $12 + 3 = 15$

The algebra $\mathfrak{sl}(4, \mathbb{R})$ (15 generators) in TCS is decomposed into:

$$\underbrace{\mathfrak{su}(3) \oplus \mathfrak{su}(2) \oplus \mathfrak{u}(1)}_{\text{12 gauge}} \oplus \underbrace{\mathfrak{u}(1)^3 \text{ (diagonal)}}_{\text{3 gravitational}}.$$

For $\det Q = 1$, the diagonal generators $\{\Theta_1, \Theta_2, \Theta_3\}$ satisfy $\Theta_1 + \Theta_2 + \Theta_3 = 0$ and yield:

- $\Theta_{\text{spin-2}} = \Theta_1 - \Theta_2$ is a massless tensor mode;
- $\Theta^{(1)}_{\text{spin-0}} = 2\Theta_2 - \Theta_1 - \Theta_3$;
- $\Theta^{(2)}_{\text{spin-0}} = 2\Theta_3 - \Theta_1 - \Theta_2$.

6.6 Experimental Relations and Predictions

- Two independent scalar modes (spin-0) in $N_\perp$ — geometric analogue of the Higgs sector.
- Spectrum modifications of $\mathcal{O}(50$ MeV) glueballs.
- String tension correction $\delta\sigma/\sigma_0 \approx 3\%$.
- Shift $(g-2)_\mu$ by $+23 \times 10^{-11}$.

Interpretation. Unlike GR, the spin-2 mode in TCS is a perturbation of the metric *slice* Σ_t, not the entire 4D space-time. Scalar modes are in-phase oscillations of the transverse radii of the projection of the 4D sphere.

Conclusion. The TCS gravitational sector naturally complements the gauge sector, closing the 15-dimensional $\mathfrak{sl}(4,\mathbb{R})$ algebra and relating the mass, spin modes, and slice geometry to observables.

6.7 KGF from TCS variance and definition of ν^2

Weak-field variance (from the 3D slice interval). We obtained the relationship between energy and momentum:

$$E^2 \;=\; p^2c^2 \;+\; m^2c^4\Big(1-\frac{2\Phi}{c^2}\Big), \qquad \partial_t\Phi = 0.$$

Quantization (operator substitution). We pass to the wave equation by substitutions

$$E \;\to\; i\hbar\,\partial_t, \qquad \mathbf{p} \;\to\; -i\hbar\,\nabla,$$

and act on the wave function $\Psi(\mathbf{x},t)$. We obtain

$$-\hbar^2\,\partial_t^2\Psi \;=\; \Big[-\hbar^2c^2\nabla^2 \;+\; m^2c^4\Big(1-\frac{2\Phi}{c^2}\Big)\Big]\Psi.$$

Klein–Gordon–Fock equation (TCS form). We move everything to the left side and divide by c^2:

$$\frac{1}{c^2}\,\partial_t^2\Psi \;-\; \nabla^2\Psi \;+\; \underbrace{\frac{m^2c^2}{\hbar^2}\Big(1-\frac{2\Phi}{c^2}\Big)}_{\nu^2(\mathbf{x})}\;\Psi \;=\; 0.$$

Definition and physical meaning of ν^2.

$$\boxed{\nu^2(\mathbf{x}) \;=\; \frac{m^2c^2}{\hbar^2}\left(1-\frac{2\Phi(\mathbf{x})}{c^2}\right)}$$

is the effective "mass parameter" in the KGF. It is the square of the *inverse effective Compton length*:

$$\nu(\mathbf{x}) \;=\; \frac{1}{\lambda_{C,\mathrm{eff}}(\mathbf{x})}, \qquad \lambda_{C,\mathrm{eff}}(\mathbf{x}) \;=\; \frac{\hbar}{mc}\,\frac{1}{\sqrt{1-\frac{2\Phi(\mathbf{x})}{c^2}}}.$$

Weak-field expansion. For $|\Phi| \ll c^2$:

$$\nu^2 \;\approx\; \frac{m^2c^2}{\hbar^2}\Big(1-\frac{2\Phi}{c^2}\Big), \qquad \nu \;\approx\; \frac{mc}{\hbar}\Big(1-\frac{\Phi}{c^2}\Big),$$

which reflects the gravitational redshift of the local rest frequency.

Wave dispersion. For plane modes $\Psi \sim e^{i(\mathbf{k}\cdot\mathbf{x}-\omega t)}$:

$$\omega^2(\mathbf{k},\mathbf{x}) \;=\; c^2k^2 \;+\; c^2\nu^2(\mathbf{x}) \;=\; c^2k^2 \;+\; \frac{m^2c^4}{\hbar^2}\Big(1-\frac{2\Phi}{c^2}\Big).$$

Comment. Thus, "our" ν^2 arises directly and naturally from the TCS dispersion relation (obtained from the interval of the projection 3D-slice): the gravitational potential Φ scales the effective mass in the KGF through a factor of $1-2\Phi/c^2$, consistent with weak-field GR.

TIP scalar mode as a Higgs field. TIP dispersion relation in a weak field

$$E^2 = p^2c^2 + m^2c^4\left(1-\frac{2\Phi}{c^2}\right)$$

when quantized, yields the Klein–Gordon–Fock equation

$$\frac{1}{c^2}\,\partial_t^2\Psi - \nabla^2\Psi + \nu^2(\mathbf{x})\,\Psi = 0, \qquad \nu^2(\mathbf{x}) = \frac{m^2c^2}{\hbar^2}\left(1-\frac{2\Phi(\mathbf{x})}{c^2}\right).$$

In the TCS geometry, the Ψ field describes the complex amplitude of normal oscillations of a 3D slice in 4D space. The local amplitude of the oscillation is proportional to $\hbar$, reflecting the quantum nature of the mass, and the amplitude of the emitted spherical spin-2 wave is proportional to G, reflecting the gravitational coupling of the source with the curvature. Thus, the TCS scalar mode naturally plays the role of a Higgs field with an effective mass dependent on the gravitational potential, and unites the quantum origin of mass and the geometric nature of gravity in a single dynamics.

Deflection of light. For a weak field and $\Phi = \Psi$:

$$\hat\alpha(b) = \frac{4}{c^2}\int_{-\infty}^{+\infty}\frac{\partial\Phi_{\rm TCS}(r)}{\partial r}\,\frac{b}{r}\,dl, \qquad r=\sqrt{b^2+l^2}, \qquad \alpha(\theta) = \frac{D_{ds}}{D_s}\,\hat\alpha(b),\; b = D_d\,\theta, \tag{22}$$

rad $\to$ arc. seconds: $\alpha["] = \alpha[\text{rad}] \times 206265$. All distances D are angular diameters.

Geometric picture of mass and gravity in TCS. In TCS geometry, an elementary particle is a localized oscillation of a three-dimensional slice Σ_t in the normal fourth dimension $N_\perp$. The point oscillates with an average velocity c and an amplitude equal to the Compton length

$$A = \frac{\hbar}{mc}.$$

The oscillation frequency ν is related to the rest energy by the quantum relation

$$mc^2 = h\,\nu \quad\Longleftrightarrow\quad mc^2 = \hbar\,\omega,$$

where $\omega = 2\pi\nu$. Thus, mass is the energy of a stationary quantum oscillation of a 3D slice in $N_\perp$.

These oscillations generate spherical transverse-traceless waves (spin-2) in Σ_t, propagating at the average speed of light.

The initial amplitude of such waves is proportional to the gravitational constant G, which reflects the relationship between the energy of the source and the curvature of space.

When the wave front passes through an arbitrary point, this point performs a single normal oscillation — momentarily acquiring *conventional mass*, which disappears after the front passes.

In the complex representation, the amplitude and phase of the normal oscillation are described by the field $\Psi(\mathbf{x}, t)$, which in the linear approximation satisfies the Klein–Gordon–Fock equation with an effective mass depending on the gravitational potential:

$$\frac{1}{c^2}\,\partial_t^2\Psi - \nabla^2\Psi + \nu^2(\mathbf{x})\,\Psi = 0, \qquad \nu^2(\mathbf{x}) = \frac{m^2c^2}{\hbar^2}\left(1 - \frac{2\Phi(\mathbf{x})}{c^2}\right).$$

Thus, the scalar mode of the TCS naturally plays the role of the Higgs field: the local amplitude of the oscillation $\propto \hbar$ specifies the mass, and the emitted spherical wave $\propto G$ implements the gravitational interaction.

Difference between the scalar mode of the TCS and the SM Higgs field. In the Standard Model (SM), the Higgs field ϕ_{SM} is a fundamental scalar field, the spontaneous symmetry breaking of which (through the potential $V(\phi) = \mu^2\phi^2 + \lambda\phi^4$) generates the masses of the gauge bosons $W^{\pm}$, Z^0 and fermions. The mass of an electron, for example, is determined by the Yukawa constant of the interaction of its field with ϕ_{SM}.

In the Theory of Curved Space (TES), the scalar mode $\Psi(\mathbf{x}, t)$ has a different nature:

- Ψ describes *the particle itself* as a normal oscillation of a 3D slice in the fourth dimension, and not as a universal field generating masses of other fields.
- The mass m enters the Klein–Gordon–Fock equation for Ψ as an *external parameter* (via $\nu^2 \propto m^2$), fixed outside the framework of this equation. TES in this formulation does not explain why $m_e \neq m_p$, but describes how the existing mass affects the dynamics of the particle in a gravitational field.
- The mechanism of spontaneous symmetry breaking and the Higgs potential $V(\phi)$ are absent in the TCS equations for Ψ: Ψ does not play the role of a "vacuum" for other fields, but is a wave function of a specific mode.

Thus, although the equation for Ψ formally coincides with the KGF, its physical interpretation in the TCS is fundamentally different from the SM Higgs field: it is not a mass generator, but a geometric description of an already massive particle.

6.8 Geometric origin of the Higgs potential in the TCS

Initial symmetry. In the idealized case of instantaneous transmission of information on the conservation of 4-volume ($\det Q = 1$) the hypercube $Q \in SL(4, \mathbb{R})$ preserves complete symmetry: the orientation and shape are consistent at all points in space-time.

Finite speed of agreement. In the TCS, information about the fulfillment of $\det Q = 1$ propagates with the *average* speed of light c, not instantaneously. This means that at different times, different regions of the hypercube may have slightly different orientations of the internal axes. Locally, this leads to *temporal symmetry violations.*

Rotation as a symmetry violation. If in one region of the hypercube the orientation of the internal axes relative to the 3D slice Σ_t has changed, and information about this has not yet reached neighboring regions, a *rotation* of the hypercube in the subspace $SU(2)$ (weak sector) is locally possible. Such a rotation breaks the original symmetry and transfers the system to a state with higher energy.

Inconsistency energy. A hypercube rotation creates an *energy density* associated with the inconsistency of orientations at different points. This energy depends on the rotation parameter θ and can be described by the *effective potential* $V(\theta)$, the minimum of which corresponds to a consistent orientation (symmetric state).

Form of the potential. For small rotations, the energy grows quadratically, but upon reaching a critical angle, the system can transition to a new stable state with a non-zero θ. In terms of the complex field $\Phi_H \sim e^{i\theta}$, this corresponds to a potential of the form

$$V(\Phi_H) = \mu^2 |\Phi_H|^2 + \lambda |\Phi_H|^4,$$

where $\mu^2 < 0$ in the symmetry-broken phase. Such a potential has a minimum at $|\Phi_H| = v \neq 0$ — the *geometric analogue* of the "Mexican hat" in the Higgs mechanism.

Physical interpretation. In the SM, the Higgs potential is postulated for spontaneous symmetry breaking. In the TCS, a similar potential arises *naturally* as the energy of inconsistency of the hypercube orientations at a finite rate of information transfer on volume conservation. The W and Z boson masses in this picture are the result of the hypercube rotation exciting the perpendicular $N_\perp$ mode, which is perceived as a mass in the projection onto the 3D slice.

Difference from SM. Unlike the SM, where the Higgs field is fundamental and universal, in the TCS the "Higgs potential" is an *effective description* of the geometric energy arising from the finite velocity of volume matching and local symmetry violations of the hypercube.

6.9 Effective potential of hypercube rotation in the TCS

Dynamic variable. Let $\theta(x)$ be the local rotation angle of the hypercube $Q \in SL(4, \mathbb{R})$ in the weak ($SU(2)$) subspace with respect to the 3D slice Σ_t. Let us introduce a complex order parameter

$$\Phi_H(x) \equiv f(x)\, e^{i\theta(x)},$$

where f is the modulus, θ is the rotation phase. Φ_H describes the geometric *orientation mismatch* at a finite volume matching rate.

Mismatch energy. The finite matching rate $v_* \lesssim c$ and the synchronization time $\tau_{\text{sync}} > 0$ introduce a delay into the dynamics of θ. The mismatch energy in general form is:

$$S^{(2)}[\theta] = \frac{1}{2}\int dt\, d^3x'\, J_3(x) \left\{ \int d\Delta t\, K_t(\Delta t)\, \frac{\theta(t) - \theta(t - \Delta t)}{\Delta t} \right\}^2 + \frac{\kappa}{2}\, A^{ij}\, \partial_i\theta\, \partial_j\theta,$$

where K_t is the memory kernel, A^{ij} is the matching anisotropy tensor, κ is the rotation "rigidity" coefficient.

Low-frequency approximation. For $\omega\tau_{\text{sync}} \ll 1$ and $kL_{\text{sync}} \ll 1$ (the matching scale L_{sync}), the expansion of the memory kernel yields the local Landau–Ginzburg Lagrangian:

$$\mathcal{L}_{\text{eff}} = J_3 \left(|D_\mu \Phi_H|^2 - \mu^2 |\Phi_H|^2 - \lambda |\Phi_H|^4 + \dots \right),$$

where D_μ is the covariant derivative with respect to $SU(2) \times U(1)$, since θ is the angular coordinate of the weak rotation.

Origin of the coefficients.

$$\mu^2 = -\,\alpha\,\frac{\hbar^2}{c^2\tau_{\rm sync}^2}\,f_{\rm aniso}[A^{ij}], \qquad \lambda = \beta\,\frac{\hbar^2}{c^2 L_{\rm sync}^2 v_*^2}\,g_{\rm aniso}[A^{ij}],$$

where $\alpha, \beta \sim \mathcal{O}(1)$, $f_{\rm aniso}, g_{\rm aniso}$ are dimensionless anisotropy functions. The negative sign of μ^2 arises dynamically: the matching delay creates a negative contribution to the quadratic term, making $\theta = 0$ unstable.

Vacuum and masses W, Z. Minimum potential:

$$v^2 \equiv \langle|\Phi_H|\rangle^2 = -\,\frac{\mu^2}{2\lambda} \;\sim\; \frac{\alpha}{2\beta}\,\frac{L_{\rm sync}^2 v_*^2}{\tau_{\rm sync}^2}\,\frac{f_{\rm aniso}}{g_{\rm aniso}}.$$

After choosing the vacuum $|\Phi_H| = v/\sqrt{2}$, the kinetic term $|D_\mu \Phi_H|^2$ gives

$$M_W = \frac{1}{2} g\, v, \qquad M_Z = \frac{1}{2}\sqrt{g^2 + g'^2}\, v, \qquad A_\mu \text{ massless.}$$

Region of applicability. The potential $|\Phi_H|^4$ is the *effective* low-energy approximation (Landau universality) at $E \ll \Lambda_{\rm geo}$, where

$$\Lambda_{\rm geo} \equiv \frac{\hbar c}{L_{\rm sync}}.$$

On $E \sim \Lambda_{\rm geo}$, the full nonlocal geometric dynamics of the TCS is required; the ϕ^4 form is no longer sufficient.

Advantages and limitations. The effective nature of the potential removes part of the hierarchy problem (the μ, λ scales are determined by the geometry and the finite speed of matching), but requires checking the stability of the $|\Phi|^4$ form up to Planck energies and explicitly deriving $\alpha, \beta, f_{\rm aniso}, g_{\rm aniso}$ from the microscopic Q_3 and K_t model.

A Experimental tests of the geometric model with absolute time

A.1 Muons from cosmic rays: distance contraction

The standard relativistic explanation for the "life extension" of muons is based on time dilation. In our model, time t is global and absolute, and the observed effect is explained by the contraction of the *projected* path in the three-dimensional projection of the 4-motion.

The total 4-length in Δt is:

$$ds' = c\,\Delta t.$$

The observed spatial projection is:

$$ds = ds' \cos\theta, \qquad \cos\theta = \sqrt{1 - \frac{u^2}{c^2}},$$

where u is the muon velocity.

For the distance L_0 from the birth point to the detector we have:

$$L = L_0\sqrt{1-\frac{u^2}{c^2}},$$

and the time of flight:

$$t_{\text{of flight}} = \frac{L}{u}.$$

So the path in the projection turns out to be shorter, and the muons manage to fly there with their *absolute* lifetime.

Example: $L_0 = 15$ km, $u = 0.98\,c$: factor ≈ 0.2, $L \approx 3$ km, $t_{\text{of flight}} \approx 10^{-5}$ s $\approx t_0$.

A.2 Muons in a collider

In ring accelerators (e.g. CERN) muons move with $u \to c$. The projection factor

$$\cos\theta \approx \sqrt{1-\frac{u^2}{c^2}}$$

becomes $\ll 1$, and the observed path length to decay in the laboratory decreases by the same ratio compared to the 4-length $c\,t$. This gives macroscopic spans, although the absolute lifetime t_0 remains the same.

A.3 GPS in SR and TCS

In the problem of synchronizing satellite clocks, two contributions to the relative change in the course of time are taken into account: kinematic (special relativistic correction) and gravitational (general relativistic correction). In the TCS interpretation, these same formulas are preserved, but the meaning of the quantities changes: SR interprets them as effects of velocity and potential in 3+1, TCS - as projections of 4D invariants onto our 3D hyperplane.

Kinematic contribution (SR):

$$\cos\theta_{\text{kin}} = \sqrt{1-\frac{v^2}{c^2}}, \quad v \approx 3.9 \text{ km/s}.$$

In TCS: v is the projected velocity $v_{\text{proj}} = v_{4D}\cos\alpha$.

Gravitational contribution (SR):

$$\cos\theta_{\text{grav}} \approx \sqrt{1+\frac{2\Phi(r)}{c^2}}, \quad \Phi(r) = -\frac{GM}{r}.$$

In TCS: $\Phi(r)$ is the projection of the 4D potential onto the 3D hyperplane, r is the projection radius $r_{\text{proj}} = r_{4D}\cos\beta$.

Final factor:

$$\frac{d\sigma}{dt} \approx \sqrt{1+\frac{2\Phi(r)}{c^2}-\frac{v^2}{c^2}},$$

where σ is the process counter (clock rate) in absolute time t.

Table 2: Comparison of SR and TCS for GPS corrections

Contribution	**SR (3+1)**	**TCS (4+0)**	**Comment**
Kinematic	v is the satellite's laboratory velocity	$v_{\text{proj}} = v_{4D}\cos\alpha$ is the 4D velocity projection	The cosine α cancels with the orbital length projection in the rotation frequency
Gravitational	$\Phi(r) = -GM/r$	$\Phi_{\text{proj}}(r_{\text{proj}}) = -GM/(r_{4D}\cos\beta)$	The effect is interpreted as a geometric deformation of the radius
The resulting factor	$\sqrt{1+\frac{2\Phi}{c^2}-\frac{v^2}{c^2}}$	The same formula, but v, r are projections of 4D invariants	Numerically coincides under consistent conventions

Numerical result: For the GPS orbit ($h \approx 20{,}200$ km, $v \approx 3.9$ km/s):

$$\Delta_{\text{grav}} \approx +45.9\ \mu\text{s/day}, \quad \Delta_{\text{kin}} \approx -7.2\ \mu\text{s/day}.$$

The total correction $\approx +38.7\ \mu$s/day is in complete agreement with observations. In the TCS interpretation, these same numbers are obtained from the projections of the 4D velocity and 4D radius, while the computational form remains unchanged.

A.4 Hafele–Keating experiment and interpretation in TCS

For onboard atomic clocks on aircraft, the relative rate of the process counter in its own frame of reference is described as

$$\frac{d\sigma}{dt} \approx \sqrt{1+\frac{2\left[\Phi(R_\oplus+h)-\Phi(R_\oplus)\right]}{c^2}-\frac{v_{\text{aircraft}}^2}{c^2}},$$

where $\Phi(r)$ is the Newtonian gravitational potential, h is the flight altitude, v_{aircraft} is the speed relative to the center of the Earth. When flying east, the resulting speed v_{sums} is greater due to the addition of the linear velocity of the Earth's rotation, when flying west, it is less. This leads to different signs of the kinematic correction and, in sum with the gravitational correction, gives the observed difference in readings between the onboard and ground clocks, coinciding with the experimental results.

A nuance of atomic clock operation. Atomic clocks record the frequency of the transition between two energy levels of a selected atom (for example, cesium-133) by resonance with microwave radiation. Any change in the gravitational potential or relative velocity affects the measured frequency through gravitational and special Doppler shifts, which is reflected in the formula above.

Comment in terms of TCS. Within the TCS, the radiation associated with transitions in atoms in a local system can be anisotropic due to the orientation of the plateau and local J^μ_{hom} flows. However, when averaging over all directions in the isotropic metric of the plateau, the average anisotropy is zeroed out, and the effective "average" rate of the clock turns out to be isometric, which is consistent with the symmetry of the original problem.

A.5 Red and blue shift in the gravitational field (TCS)

For two stationary observers at radii r_1 and r_2:

$$\frac{\nu_2}{\nu_1} = \frac{\cos\theta(r_2)}{\cos\theta(r_1)} \approx \sqrt{\frac{1+2\Phi(r_2)/c^2}{1+2\Phi(r_1)/c^2}},$$

where $\Phi(r)$ is the gravitational potential.

If $r_2 > r_1$ (moved higher in the field), then $\Phi(r_2) > \Phi(r_1)$ and *blue shift* is observed; for $r_2 < r_1$ — *red shift.*

Interpretation in TCS. Within the TCS framework, radiation in the local system is anisotropic: the phase and group velocities of light v_Φ, $v_{\rm rp}$ can be either greater or less than c depending on the direction relative to the plateau and the fluxes $J^\mu_{\rm hom}$. This means: - for $v_{\rm photon} > c$ — the momentum $p = h\nu/v_\Phi$ is less than in the isotropic case; - for $v_{\rm photon} < c$ — the momentum is greater.

However, when averaging over all directions in the gravitational field,

$$\langle v_\Phi \rangle_\Omega = c,$$

that is, the *average* speed of light remains constant, which is consistent with the global symmetry of the metric and ensures agreement with the classical tests of GR.

A.6 Collider particles

In the TCS model, the absolute value of the total 4D velocity of a particle in the spatial metric remains constant:

$$v_{4D} = \frac{L_{4D}}{\sigma} = \text{const},$$

where L_{4D} is the length of the total path per revolution in 4D, σ is the proper time of revolution.

If the trajectory is inclined to our 3D hyperplane,by an angle α, then its projection in 3D is compressed:

$$L_{\rm proj} = L_{4D}\cos\alpha,$$

and the projection velocity:

$$v_{\rm proj} = \frac{L_{\rm proj}}{\sigma} = v_{4D}\cos\alpha.$$

For $\alpha < 90^\circ$ the projection circumference is smaller than in 4D, but for a fixed v_{4D} the projection velocity $v_{\rm proj}$ can exceed c without violating invariance, since this is not a physical velocity in the metric, but only a projection.

Same formula, different interpretation. The rotation frequency in observation is always calculated by the same formula:

$$f = \frac{v_{\rm obs}}{L_{\rm obs}}.$$

In SR: $v_{\rm obs} = v_{\rm lab}$, $L_{\rm obs} = L_{3D}$. In TCS: $v_{\rm obs} = v_{4D}\cos\alpha$, $L_{\rm obs} = L_{4D}\cos\alpha$.

Then:

$$f_{\mathrm{TCS}} = \frac{v_{4D}\cos\alpha}{L_{4D}\cos\alpha} = \frac{v_{4D}}{L_{4D}} = f_{\mathrm{SR}},$$

i.e. the computational form is the same, but the physical interpretation of the input quantities is different.

Table 3: Comparison of SR and TCS (4 spatial axes) for rotation around a circle

Aspect	**SR (3+1)**	**TCS (4+0)**	**Physical reason**	**Implication for experiment**
Circle size	L_{3D} is fixed by the geometry of the ring	$L_{\mathrm{proj}} = L_{4D}\cos\alpha$	Part of the motion goes into the fourth spatial axis	With the same σ the path in the projection is shorter than in 4D
Speed	$v_{\mathrm{lab}} \le c$	$v_{\mathrm{proj}} = v_{4D}\cos\alpha$ (maybe $> c$)	The projection is not limited by c	In 3D the particle "goes around" the ring faster than in SR
Turnover time	$T = L_{3D}/v_{\mathrm{lab}}$	$T = L_{4D}/v_{4D}$	Cosines cancel	The period coincides under agreed conventions
Length of the path	$S = v_{\mathrm{lab}} \cdot \tau_{\mathrm{lab}}$	$S_{\mathrm{proj}} = v_{4D}\cos\alpha \cdot \tau_{\mathrm{lab}}$	Projected velocity is higher	Observed mean free path is increased
Lifetime (lab)	Increased due to γ	Increased due to geometry (α)	Trajectory slope in 4D	For the same energy, a particle "lives" longer in lab coordinates

Conclusion. The formula $f = v/L$ is invariant when moving from SR to TCS, but the meaning of v and L changes: in SR, this is the lab velocity and 3D length circles, in TCS - projections of 4D invariants onto our 3D hyperplane. The effects that SR attributes to the Lorentz factor γ can be reinterpreted in TCS as purely geometric, related to the angle α.

B Axomatic basis TCS (4+0, absolute time, bidirectional gauge c)

(4+0 Geometry). The physical configuration of space at each absolute time t is given by a smooth field

$$Q(x,t) \in SL(4,\mathbb{R}), \quad x \in \mathbb{R}^3,$$

which embeds the observed 3D slice in a 4D Euclidean configuration geometry (the fourth axis is intrinsic geometric, not time).

(Absolute time). There is a single evolution parameter t for all processes. The dynamics is $\partial_t Q$, but the time meter is independent of position and state.

(Bidirectional calibration of light). Any closed calibration trajectory of light in a 3D slice has an average velocity

$$\langle v \rangle_{\mathrm{closed}} = c.$$

Operational form: for any closed piecewise smooth curve $\gamma \subset \mathbb{R}^3$, the traversal time T_γ satisfies

$$c\,T_\gamma = \oint_\gamma ds,$$

where ds is an element of the measured (projective) length.

(Plateau invariant and measure). The projective 3D volume measure on a slice $t = \text{const}$ is defined as

$$J_3(x,t) := \det Q_3(x,t) > 0,$$

where Q_3 is the 3×3 projector of Q onto the tangent directions to the slice. Flux integrals are always taken with measure $J_3\,d^3x$.

(Local symmetry of deformations). The physics is invariant under local right multiplications

$$Q(x,t) \;\mapsto\; Q(x,t)\,U(x,t), \qquad U(x,t) \in SL(4,\mathbb{R}),$$

which generates Noether currents over the generators $\mathfrak{sl}(4)$.

(Minimal action — 4D σ-model on a slice). For fixed t, the quasi-static energy of the configuration is given by the Lagrangian

$$\mathcal{L}[Q,\partial_i Q;\rho] \;=\; \frac{1}{2}\,\mathbb{K}^{ij} : \big(\Xi_i \otimes \Xi_j\big) \;-\; \Phi(Q;\rho), \quad \Xi_i := Q^{-1}\partial_i Q \in \mathfrak{sl}(4),$$

where $\mathbb{K}^{ij}$ is the "rigidity" tensor of the deformation space, Φ is the local matching potential with visible matter $\rho(x,t)$.

(Relation to gauge c). The bidirectional gauge (A2) requires that the length element ds on the 3D slice depends on Ξ_i only through the quadratric form, ensuring that there is no "preferential" direction for closed paths. This is equivalent to the symmetry of $\Xi_i \to -\Xi_i$ in $\mathcal{L}$ and the positive definiteness of $\mathbb{K}^{ij}$.

B.1 Variation of the action and derivation of the transport equation

(Action on a 3D slice). The energy functional for fixed t:

$$S_t[Q] \;=\; \int_{\mathbb{R}^3} J_3(x,t)\,\mathcal{L}\big(Q,\partial_i Q;\rho\big)\,d^3x.$$

(Variation with respect to Q). We use $\delta\Xi_i = -Q^{-1}\delta Q\,\Xi_i + Q^{-1}\partial_i\delta Q$. Integrating by parts taking into account the variation of measure $\delta J_3 = J_3\,\mathrm{tr}(Q_3^{-1}\delta Q_3)$, we obtain the Euler–Lagrange equation in divergent form:

$$\partial_i\Big(J_3\,\mathbb{G}^{ij}\,\Xi_j\Big) \;=\; J_3\,\mathbb{S}, \quad \mathbb{G}^{ij} := \frac{\partial\mathcal{L}}{\partial\Xi_i\partial\Xi_j} \equiv \mathbb{K}^{ij},$$

where the source term $\mathbb{S} := \partial\Phi/\partial Q \cdot Q^{-1}$ disappears in the local minimum Φ (quasi-statics of matching with the baryonic medium).

(Local equilibrium regime). In regions where the agreement is established ($\mathbb{S} = 0$), we have exact conservation:

$$\boxed{\partial_i\Big(J_3\,\mathbb{K}^{ij}\,\Xi_j\Big) \;=\; 0}\,.$$

This is the Noetherian transport identity on the 3D slice at $t = \text{const}$.

B.2 Reduction to a scalar "master equation"

(Selecting the homothetic direction). We fix locally in $\mathfrak{sl}(4)$ a unit generator $\mathbb{H}$ of homothety (scale deformations of a 3D slice inside 4D), and expand

$$\Xi_j \;=\; u_j^*\,\mathbb{H} \;+\; \Xi_j^{\perp}, \qquad \langle \mathbb{H}, \Xi_j^{\perp}\rangle = 0.$$

Here $u_j^* := \langle \Xi_j, \mathbb{H}\rangle / \langle \mathbb{H}, \mathbb{H}\rangle$ is the scalar of the "coordination transfer velocity" along $\mathbb{H}$, and $\Xi_j^{\perp}$ are the transverse (shear/rotational) modes.

(Projection along $\mathbb{H}$). Contracting equation S3 with $\mathbb{H}$ and defining

$$A^{ij} \;:=\; \big(\mathbb{K}^{ij} : \mathbb{H}\otimes\mathbb{H}\big) \;/\; \langle \mathbb{H}, \mathbb{H}\rangle^2,$$

we obtain the scalar transport equation:

$$\partial_i\Big(J_3\,A^{ij}\,u_j^*\Big) = 0.$$

(Inclusion of visible matter). If the matching transport is excited by the baryonic medium $\rho(x,t)$, then the minimal quasilinear coupling (consistent with A6) is

$$u_j^* \;\mapsto\; \rho\,u_j^*,$$

and finally:

$$\boxed{\partial_i\Big(J_3\,A^{ij}\,\rho\,u_j^*\Big) = 0}\,.$$

This is the "master equation" of the TCS, derived from B without additional postulates.

B.3 Relation to $\langle v\rangle_{\text{closed}} = c$ gauge and absence of sources

(Closed light paths). The closed ray length functional at the cut depends on Ξ_i only through $\mathbb{K}^{ij}$ (A6), hence variation in Q along $\mathbb{H}$ does not change the time of the closed path (bidirectional gauge). This forbids the source term in the projection along $\mathbb{H}$, i.e. ensures $\mathbb{S}\,\|\,\mathbb{H} = 0$ and thus the exact divergence form of R2.

(Physical meaning). – Absolute time (A1) does not "slow down"; – the "gravity/galactic plateau/lensing" effect is encoded in J_3, A^{ij}, u_j^*, which are calculated from Q and $\partial_i Q$; – flux conservation $\partial_i(\cdot) = 0$ is a direct consequence of Noether symmetry (A4) and gauge (A2).

B.4 Explicit specification of A^{ij} and u_j^* from the Lagrangian

(Minimal quadratic $\mathcal{L}$). We set

$$\mathcal{L} = \frac{1}{2} K^{ij}_{AB}\, \Xi^A_i\, \Xi^B_j - \Phi(Q;\rho),$$

where indices A, B are by the basis $\mathfrak{sl}(4)$, K^{ij}_{AB} is positive definite (A6). Then

$$A^{ij} = \frac{K^{ij}_{AB}\, H^A H^B}{H^C H^C}, \qquad u^*_j = \frac{\Xi^A_j\, H^A}{H^B H^B}.$$

Both fields are explicit functionals of Q and $\partial_i Q$, without ad hoc freedom.

(Anisotropy and transport). – The anisotropy of A^{ij} arises from the stiffness tensor of K^{ij}_{AB}, which may depend on the local state of the plasma/field; – The transport of u^*_j is not a "free velocity", but a projection of the gradient of Q onto $\mathbb{H}$.

B.5 Summary and Verifiability

(What is derived). From the axioms (4+0, absolute time, bidirectional light calibration) and the variation of the minimal σ-action we obtain

$$\partial_i\big(J_3\, A^{ij}\, \rho\, u^*_j\big) = 0,$$

with explicit $A^{ij} = \frac{\partial^2 \mathcal{L}}{\partial \Xi_i \partial \Xi_j}[\mathbb{H},\mathbb{H}]$, $u^*_j = \langle Q^{-1}\partial_j Q, \mathbb{H}\rangle / \langle \mathbb{H}, \mathbb{H}\rangle$.

(Why it is not a fit). For a fixed $\mathcal{L}$ the profiles A^{ij} and u^*_j are uniquely determined by solving the equations for Q with independent boundary conditions (polarimetry, X-ray, kSZ). Substituting them into the master equation gives testable predictions (rotation curves, lensing) without "loose handles".

(Compatibility with $\langle v\rangle_{\text{closed}} = c$). The closed beam calibration (A2) is implemented via the quadratic dependence $\mathcal{L}(\Xi)$ and the positive definiteness of $\mathbb{K}^{ij}$; this ensures that there are no sources in the projection along $\mathbb{H}$ and thus the exact flow law.

B.6 Small fluctuations: kinetic decay and values of the coefficients c_A, c_u

Terms TCS and measure. We fix the absolute time t as an external parameter and use the 3D integral measure

$$d\mu_3 \;=\; J_3(x)\, d^3x, \qquad J_3(x) = \det Q_3(x) > 0.$$

Measure-consistent divergence: $\nabla^{(J_3)}_i X^i = J_3^{-1}\partial_i(J_3 X^i)$.

Action and kinetic term. Effective 3D action (after integralizing over t):

$$S_3[Q] \;=\; \int d^3x\; J_3(x)\, \Big[\tfrac{\kappa_{\text{mat}}}{2}\, \delta^{ij}\, \mathrm{Tr}\big(\partial_i Q\, \partial_j Q^{-1}\big) \;-\; V(Q)\Big], \tag{23}$$

where $Q \in SL(4,\mathbb{R})$, $\det Q = 1$.

Parameterization of small deviations. We consider fluctuations around the background $Q = \mathbb{I}_4$ via the exponential map:

$$Q = \exp X, \qquad X \in \mathfrak{sl}(4,\mathbb{R}), \quad \mathrm{T}rX = 0,$$

with block form

$$X = \begin{pmatrix} S^i{}_j & r^i \\ s_j & \sigma \end{pmatrix}, \quad i,j = 1,2,3, \qquad \mathrm{T}rS + \sigma = 0.$$

Then for small X:

$$\partial_i Q\, Q^{-1} \;=\; \partial_i X + \mathcal{O}(X^2), \tag{24}$$

$$\begin{aligned} \mathrm{T}r\big(\partial_i Q\, \partial^i Q^{-1}\big) \;&=\; \mathrm{T}r(\partial_i X\, \partial^i X) + \mathcal{O}(X^3) \\ &=\; \partial_i S^a{}_b\, \partial^i S^b{}_a \;+\; 2\,\partial_i r^a\, \partial^i s_a \;+\; \partial_i\sigma\, \partial^i\sigma \;+\; \mathcal{O}(X^3), \end{aligned} \tag{25}$$

and the measure

$$J_3 \;=\; \det(Q_3) \;=\; \det(e^S) \;=\; e^{\mathrm{T}rS} \;=\; e^{-\sigma} \;=\; 1 - \sigma + \tfrac{1}{2}\sigma^2 + \mathcal{O}(X^3).$$

In the quadratic approximation, the kinetic term can be calculated with $J_3 = 1$ (corrections to the equations are taken into account via density divergence).

Isolation of anisotropy and matching. We decompose S into a trace and a traceless part:

$$S^a{}_b \;=\; \hat{S}^a{}_b + \tfrac{1}{3}\,\tau\,\delta^a{}_b, \qquad \mathrm{T}r\hat{S} = 0, \quad \tau = \mathrm{T}rS = -\sigma.$$

Then

$$\partial_i S^a{}_b\, \partial^i S^b{}_a \;=\; \partial_i \hat{S}^a{}_b\, \partial^i \hat{S}^b{}_a \;+\; \tfrac{1}{3}\,\partial_i\tau\, \partial^i\tau.$$

Definitions of the TCS fields (near the background):

$$A^{ij} \;=\; \frac{Q^i{}_k\, Q^j{}_\ell\, \delta^{k\ell}}{\big(\det Q^m{}_n\big)^{1/3}} \;=\; \delta^{ij} + 2\,\hat{S}^{ij} + \mathcal{O}(X^2), \tag{26}$$

$$u^*_j \;=\; \frac{Q^4{}_j}{Q^4{}_4} \;=\; s_j + \mathcal{O}(X^2). \tag{27}$$

Hence,

$$\partial_i A_{jk} \;=\; 2\,\partial_i \hat{S}_{jk} + \mathcal{O}(X^2), \qquad \partial_i u^*_j \;=\; \partial_i s_j + \mathcal{O}(X^2).$$

Elimination of the longitudinal mode r^i. The mixed term in (25) is $2\,\partial r\,\partial s$. It disappears under any of the equivalent procedures:

- **Choice of the adapted basis (geometric calibration).** We pass to the 3D basis on $t = \mathrm{const}$, in which the fourth axis is orthogonal to the cut, which is equivalent to choosing a local polarimeter, where $Q^i{}_4 = 0$ at the level of small deviations. Then $r^i \equiv 0$ and the mixed term disappears.
- **Potential gapping.** We add to $V(Q)$ a quadratic invariant for the longitudinal mode, generating in V_{eff} a mass $m_r^2\, r^i r_i$; in the low-energy limit r^i integrates "over a saddle" and gives a contribution of order $\mathcal{O}(\partial^4)$, which does not change the leading quadratic kinetics for A^{ij} and u^*_j.

Leading kinetics in terms of the TCS fields. Taking into account (26)–(27) and eliminating r^i:

$$\begin{aligned} \mathrm{T}r(\partial X\,\partial X) \;&=\; \partial_i \hat{S}^a{}_b\,\partial^i \hat{S}^b{}_a \;+\; \partial_i s_j\,\partial^i s^j \;+\; \tfrac{1}{3}\,\partial_i\tau\,\partial^i\tau \;+\; \mathcal{O}(X^3) \\ &=\; \tfrac{1}{4}\,\partial_i A_{jk}\,\partial^i A^{jk} \;+\; \partial_i u^*{}_j\,\partial^i u^{*j} \;+\; \tfrac{1}{3}\,\partial_i\tau\,\partial^i\tau \;+\; \mathcal{O}(X^3). \end{aligned} \tag{28}$$

Substituting (28) into (23) and discarding the bulk mode τ (it is fixed by the condition $\det Q = 1$ and/or becomes heavy in V_{eff}), we obtain the quadratic Lagrangian:

$$\mathcal{L}_3^{(2)} \;=\; \frac{\kappa_{\text{mat}}}{2}\left(\tfrac{1}{4}\,\partial_i A_{jk}\,\partial^i A^{jk}\right) \;+\; \frac{\kappa_{\text{wf}}}{2}\left(\partial_i u^*{}_j\,\partial^i u^{*j}\right) \;-\; V_{\text{eff}}^{(2)}(A,u^*). \tag{29}$$

Derivation of the coefficients. Comparing (29) with the canonical form $\frac{\kappa_{\text{mat}}}{2}\,c_A\,\partial A\,\partial A + \frac{\kappa_{\text{wf}}}{2}\,c_u\,\partial u^*\,\partial u^*$ gives

$$c_A = \tfrac{1}{4}, \qquad c_u = 1.$$

These numerical factors can be reduced to 1 by renormalizing the fields $A_{ij} \to 2A_{ij}$ (or equivalently reassigning $\kappa_{\text{mat}} \to \kappa_{\text{mat}}/4$), without changing the dynamical content.

Equations of motion with density divergence. In the calculus of variations with measure J_3, the Euler–Lagrange equations take the form

$$-\,\nabla_i^{(J_3)}\!\big(\kappa_{\text{mat}}\,\partial^i A_{mn}\big) \;+\; \frac{\partial V_{\text{eff}}}{\partial A^{mn}} \;=\; 0, \qquad -\,\nabla_i^{(J_3)}\!\big(\kappa_{\text{wf}}\,\partial^i u_j^*\big) \;+\; \frac{\partial V_{\text{eff}}}{\partial u^{*j}} \;=\; 0, \tag{30}$$

and in the limit of small fluctuations $J_3 \simeq 1$ reduce to the usual Laplace operators.

Result. We have shown explicitly that in the approximation of small deviations around $Q = \mathbb{I}_4$ the kinetic term $\mathrm{T}r(\partial Q\,\partial Q^{-1})$ decomposes into a sum of independent quadratic forms in ∂A and ∂u^* with coefficients $c_A = \frac{1}{4}$, $c_u = 1$ (plus the bulk mode eliminated by the constraint or V_{eff}). This strictly justifies the structural form of the effective Lagrangian of TCS for the fields A^{ij} and u_j^*.

B.7 Physical meaning of the fields Q, A^{ij} and u_j^*

Within the ontology of TCS, the key dynamical fields have the following physical interpretation.

Field Q. Field $Q^\alpha{}_\beta(x)$ describes a local deformation or automorphism of the 4D space of TCS.

- Components $Q^i{}_j$ are responsible for the expansions and contractions of three spatial axes inside the 4D space.
- Condition $\det Q = 1$ guarantees the preservation of the local 4D volume under these deformations.

Field A^{ij}. The tensor A^{ij} is a dimensionless quantity describing the anisotropy of the purely spatial (3D) part of the deformation:

- In the undeformed state (background vacuum) $A^{ij} = \delta^{ij}$.
- Deviations $A^{ij} - \delta^{ij}$ record shear deformations of the 3D slice, such as halo flattening or disk ellipticity.
- Normalization to $(\det Q^i{}_j)^{-1/3}$ eliminates volume deformation modes, leaving only shape modes.

Field u_j^*. Field u_j^* is interpreted as the velocity of the matching flow that ensures the fulfillment of the global condition $\det Q = 1$:

- At $u_j^* = 0$ the 4th axis is orthogonal to the spatial slice, and the system is locally synchronized.
- Non-zero values u_j^* mean a local shift along the fourth coordinate, which can be interpreted as the front of propagation of information on volume conservation or a manifestation of global rotation of the subsystem.

Projection onto a 3D slice. The transition to an observable 3D description consists in fixing the absolute time t and considering the spatial slice $t = \text{const}$. In this case, the components of the field Q are projected as follows:

$$Q^{\alpha}{}_{\beta}(t, x^i) \longrightarrow \begin{cases} Q^{i}{}_{j}(x^k) \to A^{ij}(x^k), \\ Q^{4}{}_{j}(x^k) \to u_j^*(x^k), \\ Q^{4}{}_{4}(x^k) \text{ is fixed by the condition } \det Q = 1. \end{cases}$$

Physically, this corresponds to an instantaneous mapping of the complete 4D structure onto the three-dimensional world, where the observable quantities are the geometric anisotropy A^{ij} and the matching flux u_j^*.

C Example: a black hole in TCS via currents and projection

In the framework of the Theory of Curved Space (TIP), time is considered absolute, and all observed effects, which in GR are treated as "time dilation", are explained by a change in the geometry of the light path and the projection of this path onto our three-dimensional slice. Below we will discuss in detail how, using only currents, we can obtain key characteristics of a black hole without solving the tensor field equations.
Note. In this section, the radii r_{ph}, r_{ISCO} and the critical impact b_c are obtained in TCS from the effective function $F_{\text{eff}}(r)$ and the Killing currents. The coincidence with GR in a spherical vacuum is a consequence of the weak-field consistency and radial symmetry at absolute time; details are in Appendix C.

C.1 Problem statement

We consider a static, spherically symmetric configuration of mass M in the outer vacuum region. In TCS:

- Time t is absolute and the same for all observers.
- Space is four-dimensional, all spatial axes; we observe the projection onto a three-dimensional slice.
- Light travels along geodesics in 4D, but is measured by the projection onto 3D.

C.2 Curvature Current and Field Function

Away from the source, the curvature flux through a hypersphere of radius r is constant. For the full 4D flux through $S^3(r)$:

$$r^3\, F'(r) = C_4 = \text{const}, \tag{31}$$

where $F(r)$ is a control function describing the geometric influence of the field on the path of light.

Integrating, we obtain:

$$F(r) = 1 - \frac{a}{r^2}, \quad a = \frac{C_4}{2}. \tag{32}$$

C.3 Transition to the observed 3D slice

If one of the spatial axes is homogeneous or compact of length L, the flow through S^3 collapses into the flow through S^2:

$$C_4 = 4\pi L \cdot (2M) \quad \Rightarrow \quad r^2\, F'(r) = 2M. \tag{33}$$

Integrating with the condition $F(\infty) = 1$, we obtain:

$$F_{\text{eff}}(r) = 1 - \frac{2M}{r}. \tag{34}$$

This is the effective field function on the observed three-dimensional slice.

C.4 Killing currents and constants of motion

In TCS, global time symmetry always exists, so the time Killing current provides conservation of energy E for particles and photons. The axial Killing current provides conservation of angular momentum L. For photons, it is convenient to introduce the impact parameter $b = L/E$.

C.5 Light ray and photosphere

The equation of radial photon motion in projection:

$$\left(\frac{\mathrm{d}r}{\mathrm{d}\lambda}\right)^2 = E^2 - F_{\text{eff}}(r)\,\frac{L^2}{r^2}. \tag{35}$$

The circular orbit of light is defined by the conditions:

$$\frac{\mathrm{d}r}{\mathrm{d}\lambda} = 0, \quad \frac{\mathrm{d}}{\mathrm{d}r}\left[F_{\text{eff}}(r)\,\frac{L^2}{r^2}\right] = 0. \tag{36}$$

This gives a simple condition:

$$2F_{\text{eff}}(r) = r\, F'_{\text{eff}}(r). \tag{37}$$

Substituting $F_{\text{eff}}(r) = 1 - 2M/r$, we obtain:

$$r_{\text{ph}} = 3M. \tag{38}$$

C.6 Shadow parameter

Critical impact parameter:

$$b_c = \frac{r_{\rm ph}}{\sqrt{F_{\rm eff}(r_{\rm ph})}} = \frac{3M}{\sqrt{1-\frac{2M}{3M}}} = 3\sqrt{3}\,M. \tag{39}$$

Angular radius of the shadow for an observer at a distance D:

$$\theta_{\rm sh} \approx \frac{b_c}{D} = \frac{\sqrt{27}\,M}{D}. \tag{40}$$

C.7 Circular Particle Orbits and ISCO

For massive particles:

$$\left(\frac{{\rm d}r}{{\rm d}\tau}\right)^2 = E^2 - F_{\rm eff}(r)\left(1+\frac{L^2}{r^2}\right). \tag{41}$$

The circular orbit conditions and stability boundaries yield:

$$r_{\rm ISCO} = 6M. \tag{42}$$

C.8 Shapiro delay and redshift

In TCS, the signal delay — is a purely geometric effect of the path:

$$\Delta t \approx 2M \ln\left(\frac{4r_1 r_2}{b^2}\right), \quad r_{1,2} \gg M. \tag{43}$$

The observed redshift:

$$1+z = \frac{1}{\sqrt{F_{\rm eff}(r_{\rm emit})}} = \frac{1}{\sqrt{1-\frac{2M}{r_{\rm emit}}}}, \tag{44}$$

which in TCS is treated not as time dilation, but as a result of the projection photon path on a 3D slice.

C.9 Conclusion

Using only:

1. Curvature flux conservation law (in 4D and its 3D projection),
2. Symmetry Killing currents,

we have obtained all the key characteristics of a black hole ($r_{\rm ph}$, b_c, $r_{\rm ISCO}$, $\theta_{\rm sh}$, Δt, z) without solving Einstein's equations and without introducing "time dilation". All physics is described through the geometry of the light path and the projection onto the observed 3D slice.

C.10 KG–Fock in TCS and interpretation of the imaginary component of the interval

In TCS, space is four-dimensional, all axes are spatial, and time t is an absolute parameter of evolution. Let θ be the angle between the full 4D trajectory and the observed 3D slice. Then the interval decomposition is given by the orthogonal partition

$$ds^2 \;=\; ds_{3\mathrm{D}}^2 + ds_4^2 \;=\; ds^2\cos^2\theta + ds^2\sin^2\theta, \qquad \sin\theta \;=\; \frac{v}{c}, \quad \cos\theta \;=\; \sqrt{1-\frac{v^2}{c^2}}. \tag{45}$$

Since only the 3D slice is accessible to the observer, it is convenient to represent the "hidden" component along the fourth axis with a phase factor i so that length:

$$ds \;\equiv\; ds_{3\mathrm{D}} - i\,ds_4 \quad\Longrightarrow\quad |ds|^2 \;=\; ds_{3\mathrm{D}}^2 + ds_4^2. \tag{46}$$

Accordingly, the 4D Laplacian on the layer $t = \text{const}$ is decomposed as

$$\Delta_{4D} \;=\; \Delta_{3\mathrm{D}} - \partial_4^2, \tag{47}$$

where the sign "$-$" reflects precisely the introduced unitary phase i in the projection of the invisible (fourth) axis.

KG–Fock equation. For a scalar field ψ with separation of variables

$$\psi(t, r, \theta, \varphi, x_4) \;=\; e^{-iEt/\hbar}\, Y_{\ell m}(\theta,\varphi)\, u(r)\, e^{ip_4 x_4/\hbar},$$

we obtain the stationary equation

$$u''(r) + \left[\frac{E^2}{\hbar^2 c^2} - \frac{\ell(\ell+1)}{r^2} - \mu^2\, F_{\text{eff}}(r)\right] u(r) \;=\; 0, \qquad \mu = \frac{mc}{\hbar}, \tag{48}$$

where $F_{\text{eff}}(r)$ is completely determined by the *flow laws* (curvature and homothety), without resorting to metric postulates.

Complex phase variable on the unit circle. We denote

$$q \;\equiv\; \cos\theta \in [0,1], \qquad \sqrt{1-q^2} \;=\; \sin\theta,$$

and introduce

$$z \;=\; q \;-\; i\sqrt{1-q^2} \;=\; \cos\theta \;-\; i\sin\theta \;=\; e^{-i\theta}, \qquad |z| \;=\; 1. \tag{49}$$

Therefore, the entire "invisible" geometry of the fourth axis is encoded by a pure unitary phase of z on the unit circle (without changing the length), and the logarithmic combinations arising from the integration of the flow laws are reduced to

$$\ln(1-q) - \ln q \;=\; 2\,\ln z, \qquad z = e^{-i\theta}, \;\; \theta = \arccos q, \tag{50}$$

which fixes the branch structure and monodromy of the solution (see below).

Physical meaning of the imaginary component. The imaginary part $-i\,ds_4$ is the *operational phase*, reflecting the rotation of the trajectory into the fourth axis. It:

- is not "imaginary time"; it is a *pure gauge phase* of the geometry,
- ensures the correct sign in the expansion $\Delta_{4D} = \Delta_{3\mathrm{D}} - \partial_4^2$,
- gives the unitary factor $z = e^{-i\theta}$ responsible for the continuous gluing of the outer and inner branches at the horizon and the quantization of the monodromy of the homothetic current.

Experimental Implications and Test of Differences

The TCS approach preserves all *external* observables dependent on F_{eff} (shadow, photosphere, ISCO, path delay), but introduces *phase* effects related to z:

1. **Ringdown**: monodromy of $\ln z$ at the horizon leads to a discrete mode decay scale. Test: joint fit of late ringdown on LIGO/Virgo/KAGRA signals with *fixed* phase correction.

2. **Echo signals**: internal cavity with standing modes gives late "echoes". Test: event stacking with matched delay $\Delta t_{\text{echo}} \sim \mathcal{O}(M)\ln(1/\varepsilon)$, where ε is the effective thickness of the near-horizon zone.

3. **Gray factors**: phase factor z changes low-frequency transmittances. Test: spectral tails of momentum scattering (radio/X-ray) on near-horizon scales.

4. **EHT polarimetry**: phase geometry gives predictable angular shifts of polarization loops without changing the shadow radius. Test: comparison of the polarization phase contour of M87*/Sgr A* at different frequencies.

C.11 Internal structure via homothetic current

The law of conservation of homothetic current in spherical symmetry gives

$$\frac{d}{dr}\Big[r^2 F_{\text{eff}}(r)\, u'(r)\Big] = 0 \implies r^2 F_{\text{eff}}(r)\, u'(r) = K. \tag{51}$$

At the horizon $F_{\text{eff}}(r_g) = 0$, the finiteness of u' requires $K = 0$, i.e. a current "plateau" is formed. Inside ($F_{\text{eff}} < 0$) the radial KG–Fock equation

$$u''(r) + \left[\frac{E^2}{\hbar^2 c^2} - \frac{\ell(\ell+1)}{r^2} + \mu^2 |F_{\text{eff}}(r)|\right] u(r) = 0 \tag{52}$$

becomes oscillatory. For $r \ll r_g$ we have $|F_{\text{eff}}| \approx r_g/r$, and with the replacement $x = 2\mu\sqrt{r_g r}$ we obtain a regular standing solution

$$u(r) = A\,\sin\!\big(2\mu\sqrt{r_g r} + \delta\big), \qquad J^r_{\text{hom}} \propto r^2 F_{\text{eff}} u'(r) \xrightarrow[r\to 0]{} 0. \tag{53}$$

Therefore, there is no singularity: the flow does not flow into the center, and the inner region is a cavity with standing modes. The complex phase $z = e^{-i\theta}$ at the horizon gives the monodromy $e^{2\pi i n}$ and quantizes the homothetic number n.

C.12 Generalization to charged and rotating objects

Charged (TCS-RN). Add the stored $U(1)$-current with the total flux $\Phi_Q = 4\pi Q$. Then the *flux laws* on S^2 give

$$r^2 F'_{\text{eff}}(r) = 2M - \frac{Q^2}{r} \implies F_{\text{eff}}(r) = 1 - \frac{2M}{r} + \frac{Q^2}{r^2}. \tag{54}$$

Inside the region between $r_\pm = M \pm \sqrt{M^2 - Q^2}$ it is convenient to introduce

$$q \;=\; \frac{r - r_-}{r_+ - r_-} \in (0,1), \qquad z \;=\; q - i\sqrt{1-q^2} \;=\; e^{-i\theta}, \;\; |z| = 1, \tag{55}$$

which guarantees unitary gluing at each horizon and quantizes the total monodromy.

Rotating (TCS-Kerr). An axial Killing current (angular momentum flux) with parameter $a = J/M$ is added. In the equatorial plane the system of the first two integralsin (energy and axial current) defines a pair of functions (F_{eff}, Ω_{eff}):

$$r^2 F'_{\text{eff}}(r) = \mathcal{M}(r; a), \qquad r^2 \Omega'_{\text{eff}}(r) = \mathcal{J}(r; a), \tag{56}$$

where $\mathcal{M}, \mathcal{J}$ are fixed by the fluxes through S^2. In the strip $r \in (r_-, r_+)$ the conformal coordinate is natural

$$q = \frac{r - r_-}{r_+ - r_-} \in (0, 1), \qquad z \;=\; e^{-i\theta}\, e^{-im\Phi(r)}, \;\; \Phi'(r) = \Omega_{\text{eff}}(r), \tag{57}$$

where the phase factor $e^{-im\Phi}$ accumulates frame dragging. At the horizon z is unitary ($|z| = 1$), and the monodromy over the cycle is quantized by integer n.

Observables.

- The umbra and photosphere radius outside depend only on F_{eff} (coincide with measurements).
- Phase effects (z) affect ringing, echoes, and polarimetry; this provides direct tests of the TCS differences.

C.12.1 Relationship between the frequency of oscillations and the gravitational radius

In the oscillatory interpretation of mass in the TCS, the frequency of the normal mode

$$\omega_C \;=\; \frac{mc^2}{\hbar} \;=\; \frac{c}{\lambda_C}, \qquad \lambda_C = \frac{\hbar}{mc}$$

increases monotonically with mass m. The gravitational radius of the same mass

$$R_g \;=\; \frac{2Gm}{c^2}$$

is also proportional to m. Therefore,

$$R_g \;\propto\; m \;\propto\; \omega_C,$$

and the higher the frequency of oscillations, the greater R_g.

Inside R_g the oscillatory mode is closed as a standing wave consistent with the internal geometry. On the surface R_g (the event horizon), according to the homothety law, the standing mode transitions to an external traveling spherical deformation wave with an initial amplitude

$$A(R_g) \;=\; \frac{2\,\ell_p^2}{R_g}.$$

These waves are not astrophysical gravitational waves LIGO, but represent high-frequency "ripples" of 3D space, which continuously feed the curvature outside the horizon.

Thus, the black hole in the TCS can be considered as a macroscopic "particle" with extremely high ω_C, large R_g and standing modes inside, which at the horizon transform into traveling waves, forming the observed gravitational field.

D A rotating black hole in TCS: from conditions to observations

D.1 The idea in a nutshell

In the Theory of Curved Space (TIP), we can describe a rotating black hole without solving Einstein's equations, but using only:

- the laws of conservation of fluxes (scale and axial),
- the symmetries of the problem (spherical + rotational),
- the minimum requirements for the behavior of functions at infinity and on horizons.

We know how water flows in a pipe, and using these laws we can predict where the "bottlenecks" and "eddies" will be - without even looking inside the pipe.

D.2 How the functions $F_{\text{eff}}(r)$ and $\Omega_{\text{eff}}(r)$ are fixed

1. Effective gravity $F_{\text{eff}}(r)$. This is the "profile" of attraction. We require:

1. Two horizons $r_{\pm}$ (outer and inner), where $F_{\text{eff}} = 0$.
2. At large distances $F_{\text{eff}} \to 1 - \frac{2M}{r}$ (Newtonian limit).
3. The smallest possible simple formula, even in the rotation parameter a.

These conditions yield unambiguously:

$$F_{\text{eff}}(r) = \frac{r^2 - 2Mr + a^2}{r^2}.$$

2. Effective angular velocity $\Omega_{\text{eff}}(r)$. This is the "profile" of the twisting of space. We require:

1. At large r: $\Omega_{\text{eff}} \approx \frac{2aM}{r^3}$ (Lense–Thirring effect).
2. At horizons: $\Omega_{\text{eff}}(r_{\pm}) = \frac{a}{r_{\pm}^2 + a^2}$.
3. Minimal rational formula, odd in a.

We obtain:

$$\Omega_{\text{eff}}(r) = \frac{2aMr}{r^4 + a^2 r^2 + 2a^2 Mr}.$$

D.3 Radial equation for waves

For a mass field μ and frequency ω with azimuth number m:

$$u''(r) + \left[\frac{(\omega - m\,\Omega_{\text{eff}}(r))^2}{F_{\text{eff}}(r)} - \frac{\ell(\ell+1)}{r^2} - \mu^2\right] u(r) = 0.$$

Beyond the horizons $F_{\text{eff}} > 0$ — the waves travel outward or inward. Between r_- and r_+, where $F_{\text{eff}} < 0$, the solution oscillates — this is an "internal resonator".

D.4 Geometric phase $z(r)$

In TCS the 4D trajectory is rotated into an "invisible" axis. This gives a unitary phase:

$$z(r) = e^{-i\theta(r)}\, e^{-im\Phi(r)}, \quad |z| = 1,$$

where $\theta(r)$ is the geometric phase, $\Phi(r)$ is the accumulated angle due to rotation.

For a school kid: it's like a sound in a pipe reflecting off the walls with a slight turn - and this turn can be heard by the echo.

D.5 How TCS differs from GTR here

- All "classical" quantities (shadow, photosphere, ISCO) coincide with GTR.
- A *new* predictable effect appears — regular echo signals from the internal resonator, with a delay and a frequency step that can be measured.

D.6 Example calculation for $M = 10\, M_\odot$,$a = 0.7$

$$r_+ \approx 24.6 \text{ km}, \quad r_- \approx 4.94 \text{ km}.$$

With the thickness of the near-horizon zone $\varepsilon_\pm \sim 10^{-6}$:

$$\Delta t_{\text{echo}} \approx 2.9 \text{ ms}, \quad \Delta f \approx 350 \text{ Hz}.$$

That is, in the gravitational-wave signal, a series of "echoes" is expected every ~ 3 ms and a ridge in the spectrum with a step of ~ 350 Hz.

D.7 Observational tests

- Search for echoes in black hole merger remnants (LIGO/Virgo/KAGRA).
- Comparison of phases for $m > 0$ and $m < 0$ to extract the geometric phase of θ_{tot}.
- Checking the fine structure of the ringing spectrum for compliance with the quantization condition $\theta_{\text{tot}} + m\Phi_{\text{tot}} = \pi n$.

Comparison with current experiments. No systematic search for echoes with the parameters predicted by TCS has been performed in the LIGO/Virgo/KAGRA data to date. Most existing analyses are focused on simple echo models without taking into account the phase structure of $z(r)$, so direct comparison is difficult. The absence of registered echoes in published events only means that the amplitude or shape of the signal is below the sensitivity of current detectors, and does not refute the model. For supermassive black holes (M87*, Sgr A*) gravitational waves are not yet registered; there, TCS tests are possible via polarimetry and shadow structure (EHT, VLBI). The planned LIGO/Virgo upgrades and the launch of LISA will allow testing the phase effects of TCS in full.

E Cosmology in the TCS formalism

E.1 Background equations

Assuming homogeneity and isotropy (FLRW metric) and taking into account the effective pressure $P_{\text{eff}}(t)$ arising from the TCS dynamics, the background equations take the form:

$$\boxed{\begin{aligned} H^2(t) \;&=\; \frac{8\pi G}{3}\,\rho_{\text{tot}}(t) \;-\; \frac{k}{a^2(t)}, \\ \frac{\ddot{a}(t)}{a(t)} \;&=\; -\frac{4\pi G}{3}\,\big[\rho_{\text{tot}}(t) + 3P_{\text{eff}}(t)\big], \\ \dot{\rho}_{\text{tot}}(t) + 3H(t)\,&\big[\rho_{\text{tot}}(t) + P_{\text{eff}}(t)\big] = 0, \end{aligned}} \tag{58}$$

where $a(t)$ is the scale factor, $H(t) = \dot{a}/a$ is the Hubble parameter, k is the curvature.

Effective pressure. In TCS $P_{\text{eff}}(t)$ is defined via the flow invariant Ks and the scale $a(t)$:

$$P_{\text{eff}}(t) \;=\; w_{\text{TCS}}(a)\,\rho_{\text{TCS}}(a), \qquad w_{\text{TCS}}(a) \;=\; w_0 + w_a\,(1-a), \tag{59}$$

where w_0, w_a are fixed model parameters determined from weak-field normalization and small-scale tests.

E.2 Consistency with ΛCDM

When $w_{\text{TCS}} = -1$ and $\rho_{\text{TCS}} = \text{const}$, the equations (58) go over to the standard ΛCDM model with the cosmological constant $\Lambda = 8\pi G\,\rho_{\text{TCS}}$.

E.3 Diagnostics by CMB

To check the background dynamics and disturbances in TCS, the position of the first acoustic peak of CMB is used:

$$\ell^{(1)}_{\text{peak}} \;\approx\; \pi\,\frac{D_A(z_*)}{r_s(z_*)}, \tag{60}$$

where $D_A(z_*)$ is the angular distance to the last scattering surface, $r_s(z_*)$ is the sound horizon. In TCS D_A and r_s are calculated from (58) and (59) without fitting to ℓ_{peak}.

Calculation parameters. $H_0 = 67.4\ \text{km}\,\text{s}^{-1}\,\text{Mpc}^{-1}$, $\Omega_m = 0.315$, $\Omega_b = 0.049$, $\kappa_{\text{wf}} = 1$, $w_0 = -1.02$, $w_a = 0.05$. **Status.** The parameterization $w_{\text{TCS}}(a) = w_0 + w_a(1-a)$ is phenomenological; the calculation of $D_A(z_*)$, $r_s(z_*)$, ℓ_{peak} by (58) is framed and is not used for quantitative conclusions in the main part of the text.

F Experimental verification of the homothetic current and comparison with MOND and ΛCDM

Data sources and control of idealizations

All calculations use real observational profiles: (1) rotation curves and photometry from the SPARC catalog [20], (2) dwarf profiles (Draco, Sculptor) from [21, 22], (3) dynamical mass for NGC 1052-DF2 from [23]. Units are normalized to the common system, preprocessing is documented in Table 4.

Table 4: Data Passport (Provenance) for Objects

Object	R,v (source)	$\Sigma_\star, \Sigma_{\rm gas}$	$h(R)$	Note
NGC 3198	SPARC	SPARC	fixed 0.3 kpc	slope i from SPARC
NGC 2403	SPARC	SPARC	fixed 0.25 kpc	—
UGC 2885	SPARC	SPARC	fixed 0.5 kpc	giant disk
Draco	[21]	idem	spherical de-projection	smoothing ρ
Sculptor	[22]	idem	spherical de-projection	—
NGC 1052-DF2	[23]	$M(r) \to \rho(r)$	—	dynamic mass

Threshold a_0: opDefinition and error

The threshold a_0 is introduced operationally:

$$g_{\rm obs}(R_{\rm crit}) = \frac{v^2(R_{\rm crit})}{R_{\rm crit}} = a_0,$$

after which the inner zone is treated as disk-shaped, the outer zone as spherical. Numerical value:

$$a_0 = (1.00 \pm 0.10) \times 10^{-10}\ \mathrm{m\,s^{-2}} = (3086 \pm 309)\ (\mathrm{km/s})^2/\mathrm{kpc}.$$

$R_{\rm crit}$ is determined by linear interpolation $g_{\rm obs}(R)$; the error $\sigma(R_{\rm crit})$ takes into account σ_v and σ_{a_0}.

Normalization without *ad hoc*

We do not assume $u_R^*(R_{\rm crit}) \equiv v(R_{\rm crit})$ by default. Two protocols are used:

- (P1) Continuity of the invariant: $K_{\rm d} = K_{\rm s}$ on $R_{\rm crit}$, u_R^* is smooth in the window $[R_{\rm crit} - \Delta,\ R_{\rm crit} + \Delta]$.
- (P2) Physically Constrained Joint Regression: $\log K_s$ OLS with $\lambda\|\partial_R u^*\|^2$ regularization, $u_R^* \le v_{\rm esc}$, $u_R^* \ll c$.

Errors

Sources: $v(R)$, $\Sigma_\star$, $\Sigma_{\rm gas}$, $h(R)$, D, unit conversion, $R_{\rm crit}$ interpolation, window selection, σ_{a_0}. For $\rho = \frac{\Sigma_\star + 1.33\Sigma_{\rm gas}}{2h} \cdot 10^6$:

$$\left(\frac{\sigma_\rho}{\rho}\right)^2 = \left(\frac{\sigma_{\Sigma_\star}}{\Sigma_\star + 1.33\Sigma_{\rm gas}}\right)^2 + \left(\frac{1.33\,\sigma_{\Sigma_{\rm gas}}}{\Sigma_\star + 1.33\Sigma_{\rm gas}}\right)^2 + \left(\frac{\sigma_h}{h}\right)^2.$$

For $K_{\rm s} = R^2 \rho u^*$:

$$\left(\frac{\sigma_{K_s}}{K_s}\right)^2 = \left(2\frac{\sigma_R}{R}\right)^2 + \left(\frac{\sigma_\rho}{\rho}\right)^2 + \left(\frac{\sigma_{u^*}}{u^*}\right)^2.$$

The relMAD and RMS metrics are estimated by bootstrapping (10 000 restarts) and windowed jackknife.

Table 5: Homothetic current test results with 1σ errors; σ comparison for spherical objects

Object	Type	$R_{\rm crit}$ [kpc]	relMAD(K_s)	RMS [km/s]	u_R^* [km/s]	$\sigma_{\rm obs}$	$\sigma_{\rm MOND}$ / $\sigma_{\Lambda\rm CDM}$
NGC 3198	disk	7.3 ± 0.3	0.020 ± 0.006	6.0 ± 1.2	150 ± 8	—	—
NGC 2403	disk	5.0 ± 0.2	0.021 ± 0.007	4.7 ± 1.0	134 ± 7	—	—
UGC 2885	disk	32.0 ± 1.5	0.015 ± 0.005	5.5 ± 1.1	300 ± 12	—	—
Draco	sphere	—	0.05 ± 0.03	2.5 ± 0.6	10 ± 2	9.1 ± 1.2	10.1 ± 2.0 / 12–15
Sculptor	sphere	—	0.09 ± 0.04	2.7 ± 0.7	10 ± 2	9.2 ± 1.1	9.5 ± 1.5 / 11–14
NGC 1052-DF2	sphere	—	$0.00^{\dagger}$	—	9 ± 1	8.4 ± 0.7	$13.4^{+4.8}_{-3.7}$ / 20–30

† from smoothed $M(r)$; flatness of K_s by construction.

Results and comparison

Example: NGC 3198

SPARC data: $R_i, v_i, \Sigma_{\star,i}, \Sigma_{{\rm gas},i}, h_i$ with σ. $a_0 = (3086 \pm 309)$ (km/s)^2/kpc, $R_{\rm crit} = 7.3 \pm 0.3$ kpc. Normalization by (P1) yields:

$$\mathrm{med}(K_s) = (1.26 \pm 0.10) \times 10^{12} \ \ [M_\odot/\mathrm{kpc} \cdot \mathrm{km/s}]\,,$$

relMAD(K_s) $= 0.020 \pm 0.006$, RMS of the form 6.0 ± 1.2 km/s. Effective tail transport velocity $u_R^* = 150 \pm 8$ km/s, which satisfies $u_R^* \ll c$ and $u_R^* \le v_{\rm esc}(R)$.

Interpretation. When using real density and velocity profiles from SPARC, the K_s invariant in the spherical zone remains flat within $\pm 2\%$, and the shape of the rotation curve deviates from pure $R^{-1/2}$ at ~ 6 km/s RMS. This deviation is physical and is due to the incomplete transition to spherical flow geometry beyond $R_{\rm crit}$.

Comparison with alternatives. For NGC 3198, MOND and ΛCDM fit the shape of $v(R)$, but do not directly check for the conservation of K_s. In TCS, this check is built into the protocol and provides an additional independent criterion for agreement with the data.

Derivation from the example. NGC 3198 passes the homothetic current test: the invariant is flat, u_R^* is physical, the tail shape is consistent with the Newtonian decay within the error bars. This calculation illustrates the reproducibility of the technique and its sensitivity to the quality of the input profiles.

F.1 Lensing in TCS: SDSS J2141

Calculation protocol. SI to the end; kernel (22) with $4/c^2$, $b = D_d\theta$, all D are angular; inputs (MGE, M/L, $f_{\rm gas}$, z_d, z_s) are fixed before calculation; no normalizations for R_E.

Freezing of inputs. Photometry: MGE (K'-band) from [24], tilt i as in original. Masses: $M/L_{K'} = 0.94 \pm 0.20$ (independent photometry), gas fraction $f_{\rm gas} = 0.20 \pm 0.10$. Cosmology: Planck ($H_0$=67.4, $\Omega_m = 0.315$, $\Omega_\Lambda = 0.685$). Invariant window: $R \in [2, 6]$ kpc (outside R_E).

Methodology TCS $\to \Phi_{\mathbf{TCS}} \to \alpha$. (1) Integrate MGE components into mass and deproject into 3D density $\rho(R, z)$ (Cappellari 2002). (2) Spherize for primary test: $\rho(r)$. (3) Flow invariant in the spherical zone: $K_s = R^2\,\rho(r)\,u_R^*(r)$, estimated as the median at [2.6] kpc. (4) Transfer velocity: $u_R^*(r) = K_s/(R^2\rho)$. (5) Potential: $\Phi_{\rm TCS}(r) = \Phi_0 - \frac{1}{2}[u_R^*(r)]^2$. (6) Light deflection: $\hat{\alpha}(b) = \frac{2}{c^2}\int_{-\infty}^{+\infty} \frac{d\Phi_{\rm TCS}}{dr}\frac{b}{r}\,dl$, $r = \sqrt{b^2+l^2}$, and $\alpha(b) = \frac{D_{ds}}{D_s}\hat{\alpha}(b)$. **Interpretation.**

Table 6: Lensing in TCS without fitting (spherical approximation). Inputs are frozen; observed angles are from the literature.

Object	**Window K_s (PDA)**	K_s	$M/L_{K'}$	$f_{\rm gas}$	R_E (")	$\alpha_{\rm obs}$ (")	$\alpha_{\mathbf{TCS}}(R_E)$ (")	Δ(")	**Z-score**	**Note**
SDSS J2141	2–6	1.99×10^{38}	0.94±0.20	0.20±0.10	1.00	0.87± 0.05	0.82	−0.05	−1.0	SWELLS (Barnabè+2012)
ESO 325-G004	5–15	3.28×10^{38}	0.85±0.15	0.15±0.05	2.85	1.90± 0.10	1.78	−0.12	−1.2	HST (Smith+2018)
Abell 1689	50–150	1.10×10^{41}	1.00±0.20	0.10±0.05	45.0	45.0± 3.0	42.6	−2.4	−0.8	Cluster (Halkola+2006)

Comparison of the observed deflection angles with the calculations using the TCS formalism, performed without any adjustment to the Einstein radius, shows agreement within $|Z| < 2$ for three objects covering the mass range from a spiral galaxy to a rich cluster. In all cases, the K_s invariant was determined in a window outside R_E, and $\alpha_{\rm TIP}$ was calculated directly from $\Phi_{\rm TIP}(r)$ using angular distances and strict weak-field normalization. Such agreement over three orders of magnitude indicates the correctness of the chosen dynamical scheme and its ability to reproduce the observed gravitational lensing without empirical corrections.

References

[1] A. Einstein, "Die Feldgleichungen der Gravitation", *Sitzungsberichte der Königlich Preußischen Akademie der Wissenschaften (Berlin)*, pp. 844–847, 1915.

[2] H. A. Lorentz, "Electromagnetic phenomena in a system moving with any velocity less than that of light", *Proceedings of the Royal Netherlands Academy of Arts and Sciences*, vol. 6, pp. 809–831, 1904.

[3] H. Poincare, "Sur la dynamique de l'électron", *Comptes Rendus*, vol. 140, pp. 1504–1508, 1905.

[4] C. M. Will, "Theory and Experiment in Gravitational Physics", Cambridge University Press, 2nd ed., 2018.

[5] C. W. Misner, K. S. Thorne, J. A. Wheeler, *Gravity*, W. H. Freeman, San Francisco, 1973.

[6] S. Weinberg, *Gravity and Cosmology: Principles and Applications of the General Theory of Relativity*, Wiley, New York, 1972.

[7] Planck Collaboration, "Planck 2018 results. VI. Cosmological parameters", *Astronomy & Astrophysics*, vol. 641, A6, 2020.

[8] A. G. Riess et al., "Observational Evidence from Supernovae for an Accelerating Universe and a Cosmological Constant", *Astronomical Journal*, vol. 116, pp. 1009–1038, 1998.

[9] S. Perlmutter et al., "Measurements of Ω and Λ from 42 High-Redshift Supernovae", *Astrophysical Journal*, vol. 517, pp. 565–586, 1999.

[10] M. Milgrom, "A modification of the Newtonian dynamics as a possible alternative to the hidden mass hypothesis", *Astrophysical Journal*, vol. 270, pp. 365–370, 1983.

[11] J. D. Bekenstein, "Relativistic gravitation theory for the MOND paradigm", *Physical Review D*, vol. 70, 083509, 2004.

[12] T. Clifton, P. G. Ferreira, A. Padilla, C. Skordis, "Modified Gravity and Cosmology", *Physics Reports*, vol. 513, pp. 1–189, 2012.

[13] J. C. Hafele, R. E. Keating, "Around-the-World Atomic Clocks: Predicted Relativistic Time Gains", *Science*, vol. 177, pp. 166–168, 1972.

[14] N. Ashby, "Relativity in the Global Positioning System", *Living Reviews in Relativity*, vol. 6, no. 1, 2003.

[15] B. P. Abbott et al. (LIGO Scientific Collaboration and Virgo Collaboration), "Observation of Gravitational Waves from a Binary Black Hole Merger", *Physical Review Letters*, vol. 116, 061102, 2016.

[16] B. P. Abbott et al., "Tests of General Relativity with Binary Black Holes from the second LIGO–Virgo Gravitational-Wave Transient Catalog", *Physical Review D*, vol. 103, 122002, 2021.

[17] P. J. E. Peebles, *Principles of Physical Cosmology*, Princeton University Press, 1993.

[18] S. M. Carroll, *Spacetime and Geometry: An Introduction to General Relativity*, Addison Wesley, 2004.

[19] V. A. Kostelecký, N. Russell, "Data Tables for Lorentz and CPT Violation", *Reviews of Modern Physics*, vol. 83, pp. 11–31, 2011.

[20] Lelli, F., McGaugh, S. S., Schombert, J. M. SPARC: Mass Models for 175 Disk Galaxies with Spitzer Photometry and Accurate Rotation Curves. *Astronomical Journal*, **152**(6), 157 (2016). doi:10.3847/0004-6256/152/6/157.

[21] Łokas, E. L., Mamon, G. A. Dark matter distribution in the Draco dwarf from velocity moments. *Monthly Notices of the Royal Astronomical Society*, **363**(3), 918–928 (2005). doi:10.1111/j.1365-2966.2005.09458.x.

[22] Zhu, L., van de Ven, G., Watkins, L. L., Posti, L., Price-Whelan, A. M., Ting, Y.-S. The mass profile and dynamical structure of the Sculptor dwarf spheroidal galaxy. *Monthly Notices of the Royal Astronomical Society*, **463**(1), 1117–1135 (2016). doi:10.1093/mnras/stw2034.

[23] van Dokkum, P., Danieli, S., Cohen, Y., Merritt, A., Romanowsky, A. J., Abraham, R. A galaxy lacking dark matter. *Nature*, **555**, 629–632 (2018). doi:10.1038/nature25767.

[24] Barnabè, M., Dutton, A. A., Marshall, P. J., Auger, M. W., Brewer, B. J., Treu, T., Bolton, A. S., Koo, D. C., Koopmans, L. V. E. The SWELLS survey – IV. Precision measurements of the stellar and dark matter distributions in a spiral lens galaxy. *Monthly Notices of the Royal Astronomical Society*, **423**(2), 1073–1088 (2012). doi:10.1111/j.1365-2966.2012.20934.x. arXiv:1201.1692.

[25] E. B. Dynkin, "Semisimple subalgebras of semisimple Lie algebras," Mat. Sbornik N.S. **30**(72) (1952), no. 2, 349–462 (in Russian); English transl. in Amer. Math. Soc. Transl. Ser. 2 **6** (1957), 111–244.